2022

Air-Assisted Communications Using Line-of-Sight Links

Shaikha A. Alkandari
saa0017@mix.wvu.edu

Air-Assisted Communications Using Line-of-Sight Links

by

Shaikha Adel Alkandari

Thesis submitted to the
College of Engineering and Mineral Resources
at West Virginia University
in partial fulfillment of the requirements
for the degree of

Master of Science
in
Electrical Engineering

Xi Yu, Ph.D.
Xin Li , Ph.D.
Matthew C. Valenti, Ph.D., Chair

Lane Department of Computer Science and Electrical Engineering

Morgantown, West Virginia
2022

Keywords: probability Line of Sight , Poisson Point Process

Abstract

Air-Assisted Communications Using Line-of-Sight Links

by

Shaikha Adel Alkandari
Master of Science in Electrical Engineering

West Virginia University

Matthew C. Valenti, Ph.D., Chair

Recently, there has been a rapid increase in the use of air-assisted communications involving the use of airborne platforms such as unmanned aerial vehicles (UAVs). In air-assisted networks, the UAVs can act like base stations in a traditional cellular network as long as an appropriate backhaul is available. Alternatively, the UAVs could serve as relays, for instance, connecting two ground-based users who are within range of the UAV. UAVs have the benefit of being deployed and reconfigured rapidly and on demand.

Meanwhile, there has been a trend towards the use of higher and higher frequencies, including those in millimeter-wave and terahertz bands or even free-space optical communications. Such bands have the benefits of large available bandwidths, relatively little interference, and enhanced security due to spatial isolation. However, such bands are also prone to blocking in the environment, with even relatively small obstacles causing the signal to be blocked and the link unable to be closed. For such systems, successful communication requires a reliable line-of-sight (LoS) link.

When using LoS based communications, air-assisted communications is a good solution because the UAVs can be deployed sufficiently high that the ground user will likely have a line of sight or can be maneuvered to create LoS links as needed. This thesis explores the use of air-assisted communications in cluttered environments with randomized obstructions that may block the LoS between the ground user and the air platform. The key challenge is identifying blockages that are taller than a position-dependent critical height that could block the LoS of the ground-to-air link. The approach taken is to leverage tools from stochastic geometry in general, and Poisson point processes in particular, to derive a closed-form analytical expression for the probability of obtaining a LoS path in certain environments characterized as Poisson forests. An inhomogeneous Poisson point Process is used to account for the distance-dependence of the critical height, and the LoS probability is the void probability of this process. The UAV is assumed to be located at a fixed height, and its horizontal distance to the ground user could either be fixed or random. Results are verified through simulation.

Acknowledgements

I would like to show my sincere appreciation to my research advisor, Dr. Matthew Valenti. His endless knowledge, integrity, and expertise in this field have made this an inspiring experience for me. I also appreciate his time to read, through the several revisions of my work, his feedback, and the analysis he provided me to improve my thesis. I will forever appreciate his dedicated involvement, encouragement, and enthusiasm in this journey.

Furthermore, I gratefully would like to recognize my committee member, Dr. Xi Yu, for the support and guidance she has provided me. In addition, I would like to thank my committee member, Dr. Xin Li, for his knowledge, and appreciation.

I am very fortunate to have my greatest source of inspiration and never-ending support along this journey, my parents. They have been showing an overwhelming amount of support and love since the day I decided to pursue my master's degree. I am also eternally thankful for my sisters, brother, and friends who also have been a source of motivation throughout this milestone. Moreover, this endeavor would not have been possible without the unconditional love and support of my grandfather, who inspired me to achieve the dreams I once aspired to accomplish. I am incredibly blessed to be a part of your lives and thank you for making this possible.

Contents

List of Figures

List of Tables

Notation

We use the following notation and symbols throughout this thesis.

BS	base station
cdf	cumulative distribution function
LoS	line-of-sight
mmWave	millimeter-wave
pdf	probability density function
PPP	Poisson point process
QoS	Quality of Service
SINR	signal-to-interference-and-noise ratio
SNR	signal-to-noise ratio
UAV	unmanned aerial vehicle

Chapter 1

Introduction

1.1 Aerial Communication

Unmanned aerial vehicles (UAVs) also known as drones, are known for their high mobility and low cost. UAVs can come in different sizes, such that smaller UAVs can be easily reachable in different environments, and applications such as weather forecasting[1].

UAVs could be efficiently deployed to support cellular networks and enhance their quality-of-service (QoS). [2, 3]. It is possible to boost wireless capacity and coverage during temporary events or hot areas such as outdoor sporting events by using airborne base stations based on UAV aircraft [3, 4].The flexibility of UAV systems for on-demand deployment is considered as an advantage for urgent matters such as sensing the forest fire [1]. In addition, when terrestrial networks are damaged, they may enable disaster assistance and offer communications for public safety [5].

The variety of UAV sizes and features have created number of interesting research problems. For instance, researchers have studied the use of smaller battery powered UAVs that could be beneficial for air to ground communications. Additionally, the smaller UAVs have different characteristics compared to normal UAVs, owing primarily to their distinct physical embodiments [5].

Moreover, UAVs in a network can play different roles and could potentially solve the weaknesses found in wireless networks. Hence, one of the important roles studied is using the UAVs as flying base stations (BSs) [3]. For high density areas where complications

could potentially occur in communication infrastructure, UAVs are beneficial and promising in supporting broadband wireless [5]. In addition, a flying base station helps to improve coverage, efficiency, and deliver the requested service, which enhances the user's quality of experience [6].

The location of the BS, mobility, power consumption, and development of recharging solutions are some of the difficulties associated with deploying aerial BSs. Due to the UAVs' placement at various heights, which may affect coverage and the up-link and down-link channels, placement is regarded as a problem.Because there are terrestrial BSs nearby where there are aerial BSs, there may be interference. Moreover, a UAV BS position can also be altered, although doing so would result in a loss of service time because of the need to move. The short battery life of aerial BSs, which is drained by mobility and electronics, is one of its drawbacks. The cost of replacing the UAV BSs repeatedly with fully charged ones would be incurred once the battery of the aerial BSs runs out and needs to be recharged [6].

Although UAVs aid in increasing capacity, the framework still needs to be designed optimally in order to manage resources like bandwidth, energy, and power transmission to serve ground users. Considering UAV BSs mobility and the fluctuating traffic patterns of ground users, resource management could be difficult. Effective scheduling is necessary to prevent idle resources and duplicate schedules because of terrestrial base stations [7].

One common attribute of UAVs is their flexibility and mobility [8]. Various studies have focused on communication using Line-of-Signt (LoS) links between ground to air links. Such LoS links are characteristic of broadband links that make use of ever higher frequencies, such as millimeter-wave and terahertz bands or even free-space optical communications.

It is worth mentioning that one of the key benefits of using UAVs as flying BS is their suitability for LoS environments, as quantified by a high probability of a LoS path [5].

LoS connections are prone to blocking by obstructions such as trees in a forest or buildings in a city. Modelling a cellular network in urban areas is particularly challenging due to the potential blocking from buildings. Such a scenario was considered in [9], where the UAVs are deployed within the city at random locations but at a fixed height. By using results from stochastic geometry, the optimal height was found for various environments as a function of the number of UAVs deployed per unit area.

In addition to serving as base stations within a traditional infrastructure-based network, UAVs can serve as relays or intermediate nodes in ad hoc networks that may lack a dedicated infrastructure. Such applications are particularly useful when two users located on the ground wish to communicate, but cannot due having poor propagation conditions, such as a blocked LoS path. By positioning a UAV at an appropriate location, both users may be able to simultaneously see the UAV despite not being able to see each other. The UAV can therefore be used as a relay. The idea can be extrapolated to networks with multiple UAVs serving multiple ground users. Wireless network deploying multiple UAVs acting as relays can provide better coverage and connectivity with the ground network [10].

1.2 Line of Sight and mmWave Communications

Over the past decades, wireless networks have evolved from 1G cellular networks operating over limited bandwidth to today's broadband 5G systems. This technological advance has been accompanied by a massive increase in the usage of mobile data and smartphones. This has left wireless providers with the challenge of facing a shortage of bandwidth [11]. Cellular operators strive to offer low-latency, high-quality videos, and multimedia services. Until only recently, providers have had to provide service over carrier frequency bands of 700 MHz to 2.6 GHz[11].

This increase in demand for mobile data service can be met through the use of new spectrum being opened up in millimeter wave (mmWave) bands. Millimeter wave has been the subject of a number of studies that highlight both its advantages and its drawbacks. Researchers have found that employing mmWave allows for unprecedented high data rates. However, to overcome the severe path losses at mmWave, advanced antenna arrays are required, such as those that can quickly execute beamforming training and tracking [12].

The implementation of mmWave is having a positive impact on microcellular networks. Such networks could deploy compact arrays with a massive number of antennas at both transmitter and receiver, though form-factor limitations will generally dictate that the base station can have many more antennas than the mobiles it serves. Additionally, mmWave offers high data rate and low latency to allow better communication between devices in mobile

networks such as those in vehicles. Increasing the efficiency of mobile networks, especially those in urban settings, will allow for enhanced communication in vehicle-to-infrastructure settings [12]. Another consideration for the use of mmWave communications is the need for better techniques for backhauling signals [11]. Furthermore, as a well-known feature of mmWave is their large bandwidth, a positive aspect behind them is having a shorter delay spread which has an impact on equalization [13].

Although there lots of advantages of mmWave, they tend to be vulnerable to obstructions and blocking. This is due to three reasons. The first reason is due to their high penetration loss when impinging materials like concrete and tinted glass because of their smaller wavelength. The second reason is the fact that mmWave lengths are smaller than objects which causes them to bend, thereby increasing diffraction effects. Lastly, one of the most key features of mmWave is its large bandwidth, but this comes with low transmit powers and hardware limitations which results in a disadvantage in the Signal-to-noise ratio (SNR) regardless of antenna gains, hence they do not tolerate blocking well [13].

UAVs are well suited to be applied in cellular networks operating at mmWave frequencies and therefore are subjected to blockages. This is because the UAVs can be deployed sufficiently high that the ground user will likely have a line of sight or can be maneuvered to create LoS links as needed. For such systems, it is important to be able to characterize the link between the ground user and the UAV in the air. This characterization can be done quantitatively in terms of a LoS probability, i.e., the likelihood that a part between a ground user and a UAV is LoS and therefore not blocked by an obstruction. The amount of blockages depends on the environment, for instance if it is urban, suburban, rural, or a forest. In addition to the location of the blockages, their heights are important factor, as are the distances between the two devices and the heights of the ground user and UAV [14].

1.3 Utilizing Stochastic Geometry in Modern Networks

The modelling of modern wireless networks requires a mathematical approach that is effective in terms of methodology and application. In this regard, stochastic geometry is a preferred approach for such networks [15]. The specific tools within the field of stochastic

geometry are critical in the analysis of coverage, outage, and rate of wireless networks. The key assumption with stochastic geometry is that the location of blockages and communication devices are drawn from an appropriate point process [9]. Researchers have recently focused on using stochastic geometry to examine the system-level performance of mmWave cellular networks, which is driven by the mathematical flexibility of the Poisson point process (PPP) based abstraction modeling [16].

Transceiver nodes in stochastic geometry are modeled on a random basis within a network provided they are located in the 2-D plane and can form intensity and ensure the spread of interferers. Stochastic geometry permits the derivations of analytics that can guarantee average performance metrics such as the spectral efficiency, signal-to-interference-and-noise ratio (SINR), and sum of throughput appropriate for infinite networks. A study that was conducted in the framework of mmWave-based cellular systems. The study relied on the results derived from stochastic geometry to distinguish network capacity and coverage [15]. Essential propagation elements of mmWave signal and in particular human body and buildings were considered as some of the blockage sources for modelling. A distance-oriented blockage model was first deduced based on the results guided by the random shape theory, which was later applied to deduce analytic expressions for Signal to Interference and Noise Ratio (SINR) coverage [17] one assumption that was considered important for the derivations was that the source of signal blockages was based on independent Poisson Point Processes (PPP). Stochastic geometry methods could be used also in including the features of mmWave cellular network [18] where the study is heavily emphasized on downlink coverage analysis on small cell network.

It is important to note that in the case of dense indoor activities using mmWave, human bodies are considered the key source of blockages that give attenuation in the range of 30-60 dB for mmWave signals. Users who carry or posses devices that have the potential to interfere can also block the interference that can come from other users. This makes the major distinction between indoor mmWave systems and the outdoor cellular systems [19]. The other difference between the two systems stems from the number of transceiver devices and the spatial extent considered during analysis. In as much as infinite number of users could be verified and infinite region of operation could be considered, system models must

accommodate the number of users and finite geometry [20]. The consideration was vital for generating insight into the type of surface reflections that occur in the setting of indoor mmWave setup. Prior work that focused on mmWave-based networks relied on the results derived from stochastic geometry in the analysis of rate and coverage while at the same time modelling the effect of blockages and the direction of antennas[21]. For purpose of ensuring tractability of analysis, most experiments are done on the assumption of infinite number of usable mobile devices distributed in an infinite region. The assumptions are useful in analytical expressions and utilization of Campbell's theorem. In urban settings, mmWave are utilized to avail enormous amounts of bandwiths [20].

1.4 Thesis Outline

This thesis explores the use of air-assisted communications in cluttered environments with randomized obstructions that may block the LoS between the ground user and the air platform. The key challenge is identifying blockages that are taller than a position-dependent critical height that could block the LoS of the ground-to-air link. The approach taken is to leverage tools from stochastic geometry in general, and Poisson point processes in particular, to derive a closed-form analytical expression for the probability of obtaining a LoS path in certain environments characterized as Poisson forests. An inhomogeneous Poisson point Process is used to account for the distance-dependence of the critical height, and the LoS probability is the void probability of this process. The UAV is assumed to be located at a fixed height, and its horizontal distance to the ground user could either be fixed or random. Results are verified through simulation.

The remainder of this thesis is organized as follows. In Chapter 2, we derive the LoS probability for the ground-to-air channel when all of the devices are in fixed locations and the environment is a Poisson forest. Closed-form solutions are provided for two distributions for the heights of the obstructions: uniform and truncated Gaussian. Next, in Chapter 3, we explore the use of air-assisted communication to help connect two ground users via a centrally located UAV acting as a relay. Chapter 4 extends the analysis of a fixed network to one where the UAV may be randomly located. Results are given for two distance distributions:

uniform and exponential. Finally, the thesis concludes in Chapter 5, where some ideas for future work are presented.

Chapter 2

Line-of-Sight Prediction for the Ground-Air Channel

2.1 System Model

Consider the network shown in Fig. 2.1 consisting of a user located at the ground at a height of h_g, a UAV with a fixed location along the horizontal line x_a positioned with an altitude or height h_a, and objects that are potential sources of blockage (*e.g.*, trees) of a non-trivial thickness. The potential blockages are drawn from a one-dimensional Poisson Point Process (PPP) of density λ_0 . The number of potential blockages along the horizontal line from the ground user to the shadow of the UAV is equal to N, where N is a Poisson random variable as explained in the next section. The location of each potential blockage is a random variable $B_k, k \in \{1, ...N\}$, and the height of each potential blockage is also a random variable H_k. Due to being drawn from a PPP, the N locations B_k are independently distributed according to a uniform distribution as explained in the next section. It is assumed that the heights of the N potential blockages are independent and identically distributed (i.i.d.) and that their cumulative distribution function (cdf) is $F_H(h)$. The heights may be drawn from different distributions, for instance they may be uniformly distributed or distributed according to a (truncated) Gaussian. A potential blockage is an actual blockage if it blocks the LoS path, which will only occur if the blockage is sufficiently high, as will be discussed later in this chapter.

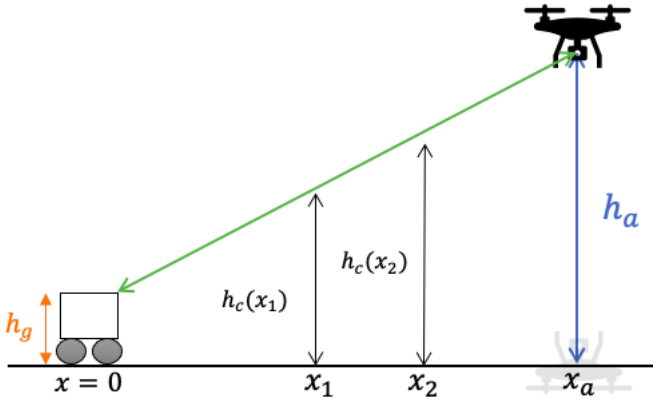

Figure 2.1: Example of one dimensional aerial network consisting of a UAV, a ground user, and potential blockages. Two black lines indicates potential blockages that will become actual blockages if they are above the corresponding critical heights indicated by the green line, which also indicates the LoS path from the ground user to the UAV. The orange line indicates the height of the ground user's antenna. The blue line indicates the height of the UAV, while the shadow of the UAV shows the location of the UAV on the horizontal coordinate.

2.2 Poisson Point Processes

Poisson point processes have several key properties that make them convenient to analyze. In particular, the number of points within a given region is a Poisson random variable, the locations of the points within the region are independent and identically distributed, and the number of points in two disjoint regions are independent. PPPs find many applications in communications, including their use in characterizing interference arising from randomly located interfering transmitters [22, 23].

PPPs can be defined for any number of dimensions. For the present application, the altitude of the UAV and the height of the ground antenna are fixed, so there is no randomness in the vertical dimension. Thus, the problem may be characterized by at most two dimensions. However, since this thesis considers just one communication link at a time, the problem may be collapsed into just one dimension, where that one dimension is the line drawn on the ground plane between the transmitter and receiver. The purpose of this section is to review some results related to one-dimensional PPPs.

Let N represent the number of points in a one-dimensional PPP contained within some

interval with a finite length ℓ. From the properties of a PPP, the variable N is a Poisson random variable. Letting μ represent the mean value of N, then the probability mass function of N is given by [24]

$$\mathbb{P}\{N = n\} \quad = \quad \frac{\mu^n}{n!} e^{-\mu}. \tag{2.1}$$

PPPs may be either *homogeneous* or *inhomogeneous*. A *homogeneous* PPP is characterized by an *intensity*, also sometimes called a *density*, denoted by the fixed scalar value λ, which represents the expected number of points within a unit-length interval. For a homogeneous PPP, the value of μ in (2.1) is simply the density λ multiplied by the length of the interval ℓ

$$\mu \quad = \quad \lambda\ell. \tag{2.2}$$

It is noted that for a homogeneous PPP, the N points are all uniformly distributed within the interval. Thus, a straightforward way to realize a PPP is to use a two-step procedure, where the first step involves drawing the value N from a Poisson distribution, and then the second step involves independently dropping N points over the interval with each point's location being a uniform variable matched to the width of the interval.

Inhomogeneous PPPS, sometimes called *nonhomogeneous* PPPs, are characterized by an *intensity function* $\lambda(x)$ that depends on location along the one-dimensional coordinate x. Inhomogeneous PPPs can be used to characterize point processes where the points are more likely to be in some locations than others. For an inhomogeneous PPP, the value of μ in (2.1) is found by integrating the intensity function over the interval

$$\mu \quad = \quad \int_0^\ell \lambda(x) dx \tag{2.3}$$

where in the above integral it is assumed without loss of generality that the coordinates are chosen such that the interval starts at the origin. As with homogeneous PPPs, the number of points in an interval for an inhomogeneous PPP is a Poisson random variable and its pmf is given by (2.1). An inhomogeneous PPP can also be realized through a two-step procedure involving drawing N from a Poission distributon and then independently dropping N points. However, care must be taken to make sure the points are dropped according to the

appropriate distribution which will generally not be uniform. Obviously, an inhomogeneous PPP collapses to a homogeneous PPP when the intensity function is constant $\lambda(x) = \lambda$, in which case the integral of (2.3) evaluates to (2.2).

In this work, special attention is made to the probability that $N = 0$; i.e., that there are no points within the interval. For instance, if the points represent blockages, then the probability that $N = 0$ becomes the probability that there are no blockages in the region, which is a probability called the Line-of-Sight (LoS) probability in this thesis. This probability is found by evaluating (2.1) for $n = 0$

$$\mathbb{P}\{N = 0\} = \frac{\mu^0}{0!}e^{-\mu} = e^{-\mu}. \tag{2.4}$$

The above probability is called the *void* probability of the PPP.

2.3 LoS Probability

The LoS probability is the probability of having an unblocked link between the ground user to the fixed UAV in the air. The LoS probability depends on how potential blockages are distributed along the straight line from the ground user ($x = 0$) to the UAV ($x = x_a$), which are modeled as a Poisson process with density λ_0. Each potential blockage may block the LoS between the ground users to the UAV depending on its height and its location along the horizontal line. The *critical height* is the height above which a potential blockage becomes an actual blockage, because if it is higher than this value then the LoS path will be blocked. The critical height is determined by linearly interpolating the straight line that connects the ground antenna to the UAV over the interval $(0, x_a)$. This linear interpolation is found by noting that this straight line has a slope of $(h_a - h_g)/x_a$, which is the rise over the run as shown in Figure 2.1.

Therefore, the critical height will be a function of the location $x \in [0, x_a]$ along the horizontal coordinate, and is given by:

$$h_c(x) = \frac{h_a - h_g}{x_a}x + h_g. \tag{2.5}$$

Notice that $h_c(x)$ increases linearly with x.

Table 2.1: Summary of Notations

Notations	Description
λ_0	Density of Blockages
x_a	Horizontal distance to the UAV
h_g	Height of the ground user
h_a	Height of the UAV
h_{max}	Maximum height of the Blockage

For the special case that $h_a = h_g$, the critical height will be a constant value h_c. Since not all blockages are tall enough to block the LoS between the ground user and UAV, only those potential blockages that are higher than h_c will actually block the LoS. For any random potential blockage, the probability that it has a height h_0 greater than h_c is found using its cdf as follows:

$$\mathbb{P}\{h_o > h_c\} = 1 - F_H(h_c). \tag{2.6}$$

Therefore, the distribution of blockages with heights greater than h_c in this Poisson forest can be modeled as a homogeneous Poisson process with density λ_c defined as:

$$\lambda_c = \lambda_0 \mathbb{P}\{h_o > h_c\} = \lambda_0 \left[1 - F_H\left(h_c\right)\right]. \tag{2.7}$$

When $h_a \neq h_g$, the critical height becomes location-dependent as in (2.5). In this case, this model becomes an inhomogeneous Poisson process with a location-dependent intensity $\lambda(x)$ defined as:

$$\lambda(x) = \lambda_0 \left[1 - F_H\left(h_c\left(x\right)\right)\right]. \tag{2.8}$$

Since $F_H(\cdot)$ is a monotonically increasing function, $\lambda(x)$ decreases monotonically as h increases. Thus, for a given UVA location, the PPP is denser closer to the origin, since the objects closer to the origin are more likely to block the LoS than objects that are closer to the UAV.

As defined in (2.8) the distribution of the blockages that are tall enough to disrupt the unobstructed view fits an inhomogeneous Poisson process with a location-dependent density. The probability of having no blockages obstructing the LoS between the ground user located at 0 to the UAV located at x_a is found by the void probability of the inhomogeneous PPP,

which from (2.3) and (2.4) is as follows:

$$\mathbb{P}_{LoS}^{ga}(x) = \exp\left(-\int_0^{x_a} \lambda(x)dx\right). \tag{2.9}$$

Finding a solution to (2.9) depends on the difficulty of performing the integration, which depends on the nature of $F_H(h)$. In some cases, such as the two examples provided below, closed-form solutions can be found. Alternatively, when closed-form solutions cannot be readily obtained, (2.9) can be solved numerically, for instance, by using numerical integration. Table 2.1 shows a list of notation used in this chapter.

2.4 Analysis of Uniform Random Height Distributions

2.4.1 Derivation of Closed-form Expression

Consider the case that the heights of the blockages are uniformly distributed with maximum height of h_{max}. The cdf used in (2.8) is

$$F_H(h) = \begin{cases} 0 & \text{for } h < 0 \\ \dfrac{h}{h_{\max}} & \text{for } 0 \le h \le h_{\max} \\ 1 & \text{for } h > h_{\max} \end{cases}, \tag{2.10}$$

For the uniform distribution, the density of the inhomogenous PPP is given by (2.8), where $F_H(\cdot)$ is given by (2.10) and $h_c(\cdot)$ is again given in (2.5).

Evaluating $F_H(h_c(x))$ we obtain

$$F_H(h_c(x)) = \begin{cases} 0 & \text{for } x \le x' \\ \left(\dfrac{h_a - h_g}{x_a h_{\max}}\right) x + \dfrac{h_g}{h_{\max}} & \text{for } x' < x \le x_c \\ 1 & \text{for } x > x_c \end{cases} \tag{2.11}$$

Where x' is

$$x' = \frac{-h_g x_a}{(h_a - h_g)} \tag{2.12}$$

The variable x_c is the *critical distance* at which any potential blockage at a further distance ($x > x_c$) cannot block the LoS since $h_c(x) > h_{\max}$ over this range. This distance is given by:

$$x_c = \left(\frac{h_{\max} - h_g}{h_a - h_g}\right) x_a. \tag{2.13}$$

Since x' is negative for the usual case that $h_a > h_g$, it is inconsequential owing to the fact that the integral of (2.9) does not cover negative x. The density of the inhomogeneous PPP is found by substituting (2.11) into (2.8) resulting in:

$$\lambda(x) = \begin{cases} \lambda_0 \left[1 - \left(\dfrac{h_a - h_g}{x_a h_{\max}}\right) x - \dfrac{h_g}{h_{\max}}\right] & \text{for } 0 < x \leq x_c \\ 0 & \text{for } x > x_c. \end{cases} \tag{2.14}$$

From (2.9), $\mathbb{P}_{LoS}^{ga}(x_a)$ requires that $\lambda(x)$ be integrated from 0 to x_a. If $x_a \leq x_c$, then

$$\int_0^{x_a} \lambda(x)dx = \int_0^{x_a} \lambda_0 \left[1 - \left(\frac{h_a - h_g}{x_a h_{\max}}\right) x - \frac{h_g}{h_{\max}}\right] dx. \tag{2.15}$$

When $x_a > x_c$, $\lambda(x) = 0$ for $x > x_c$ and thus the integral from x_c to x_a is zero. It follows then that the integral will take the same form as in (2.15) but the upper limit can be tightened to x_c since the integral beyond that point is zero.

Rather than expressing the integral separately for the two cases of $x_a \leq x_c$ and $x_a > x_c$, we can express them as the following single expression

$$\int_0^{x_a} \lambda(x)dx = \lambda_0 \int_0^{\min(x_a, x_c)} \left[1 - \left(\frac{h_a - h_g}{x_a h_{\max}}\right) x - \frac{h_g}{h_{\max}}\right] dx. \tag{2.16}$$

Defining λ_u as the solution of the previous integral we have

$$\lambda_u = \int_0^{x_a} \lambda(x)dx = \lambda_0 \min(x_a, x_c) \left[1 - \frac{h_g}{h_{\max}} - \left(\frac{h_a - h_g}{2x_a h_{\max}}\right) \min(x_a, x_c)\right]. \tag{2.17}$$

Then, using λ_u we get that the probability of obtaining LoS for ground-air communication $\mathbb{P}_{LoS}^{ga}$ at $x = x_a$ is given by

$$\mathbb{P}_{LoS}^{ga}(x_a) = e^{-\lambda_u}. \tag{2.18}$$

from (2.17), we can obtain closed expression for $\mathbb{P}_{LoS}^{ga}$ and substitute λ_u in (2.18) The $\mathbb{P}_{LoS}^{ga}$ can be rewritten as

$$\mathbb{P}_{LoS}^{ga}(x_a) = e^{-\lambda_0 \min(x_a, x_c)\left[1 - \frac{h_g}{h_{\max}} - \left(\frac{h_a - h_g}{2x_a h_{\max}}\right) \min(x_a, x_c)\right]}. \tag{2.19}$$

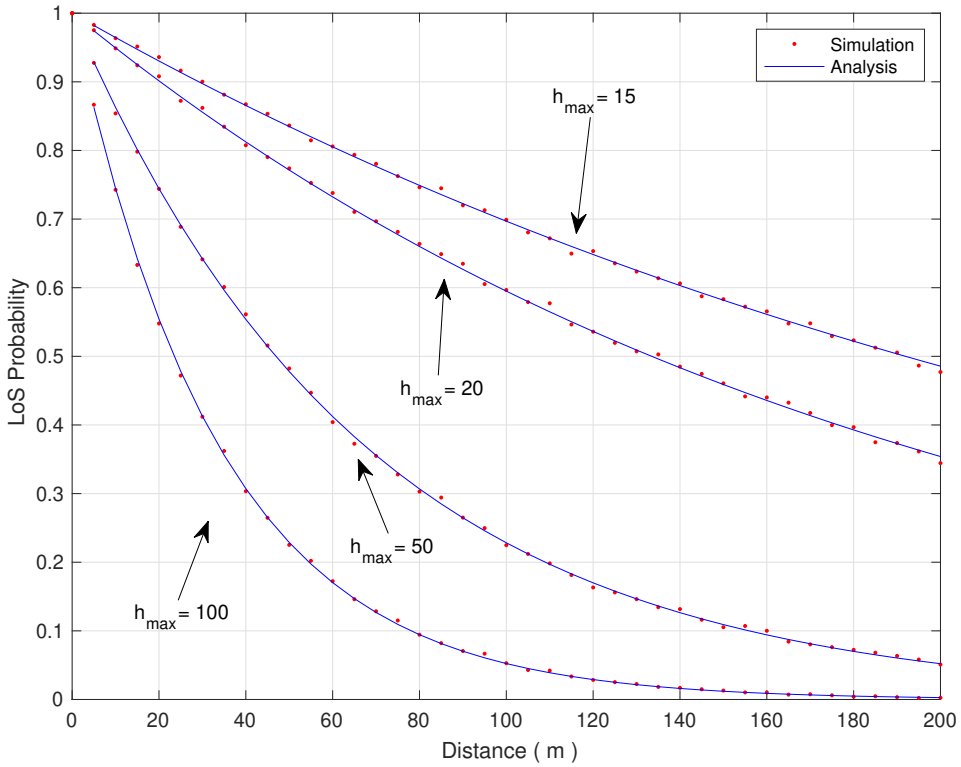

Figure 2.2: Probability of obtaining LoS from a ground user located at 0 and to an UAV located at x_a for a Uniform height distribution and $h_g = 2m$. Solid lines show the numerical results calculated using our closed-form expressions, while the dots show results generated by Monte Carlo simulation.

2.4.2 Simulation and Analysis Validation

In this section, we present numerical results generated by our methods. The key part of these methods is the calculation of the probability of obtaining a LoS between the ground user and the UAV. We consider a Poisson forest where the locations of the obstacles along a straight line are generated via a Poisson point process with $\lambda_0 = 0.05$. The distributions of the obstacle height H_t were chosen to be a uniform distribution with cdf $F_H(h)$ defined as in (2.11).

To validate the numerical results, we performed Monte Carlo simulations involving the repeated drawing of Poisson forests. Let ℓ be the interval of a simulated Poisson forest, where $\ell = x_a$ for a ground user to UAV link. Drawing a Poisson forest involves first determining the random number N of blockages in the interval, which is done by drawing N from a

Poisson distribution of mean $\lambda_0 \ell$. Next, each of the N blockages is placed uniformly over the interval. Then, each blockage's height is determined by randomly drawing its H from the corresponding distribution. Once the forest was constructed, it was determined whether or not the LoS path was blocked by checking to see if any of the blockages were above the critical height at that location. This process was repeated for 10 thousand trials for each data point reported.

Figure 2.2 shows the probability of obtaining LoS between a ground user and UAV, $\mathbb{P}LoS^{ga}(x)$, with the horizontal distance x_a. In this figure, the blockages are distributed from a random uniform distribution. We are varying the the blockage's maximum height $h_{max} = [15, 20, 50, 100]$ (m). The UAV flies at to a fixed heights of $h_a = 80$ meters. The ground user has a communication device fixed at the height of $h_g = 2$ meters. The results in figure 2.2 indicates that $\mathbb{P}^{ga}_{LoS}(x)$ decreases as x_a increases. That reason behind is straightforward. A longer distance between the ground user and the UAV will allow a greater probability of having blockages between. However, $\mathbb{P}^{ga}_{LoS}(x)$ increases as h_{max} decreases. This is because increasing the value of the blockage's height h_{max} will results to high chances of h_{max} to be greater than the critical height. Therefore, the taller the blockages height are the more likely it will be blocked which decreases the chance of obtaining the LoS probability.

Figure 2.3 shows the probability of obtaining LoS between a ground user and UAV, $\mathbb{P}LoS^{ga}(x)$, with the horizontal distance x_a. In this figure we parameterized over different UAV heights h_a. The the blockage's maximum height is set at $h_{max} = 20$ (m). The UAV flies with different altitudes of $h_a = [10, 20, 50, 100]$ meters. The ground user has a communication device fixed at the height of $h_g = 2$. The results shows that $\mathbb{P}^{ga}_{LoS}(x)$ increases as h_a increases. This is because the critical height will increase with a greater h_a (as in (2.5)). As the critical height gets higher it will potentially increases the probability of obtaining LoS. That is because when the critical height increases the blockages height will most likely decreases.

Figure 2.4 shows the probability of obtaining LoS between a ground user and UAV, $\mathbb{P}LoS^{ga}(x)$, with the horizontal distance x_a. In this figure we parameterized over different density λ_0. The the blockage's maximum height is set at $h_{max} = 20$ meters. The UAV flies with the altitudes of $h_a = 80$ meters. The ground user has a communication device fixed at the height of $h_g = 2$. The results shows that $\mathbb{P}^{ga}_{LoS}(x)$ decreases as λ_0 increases since there

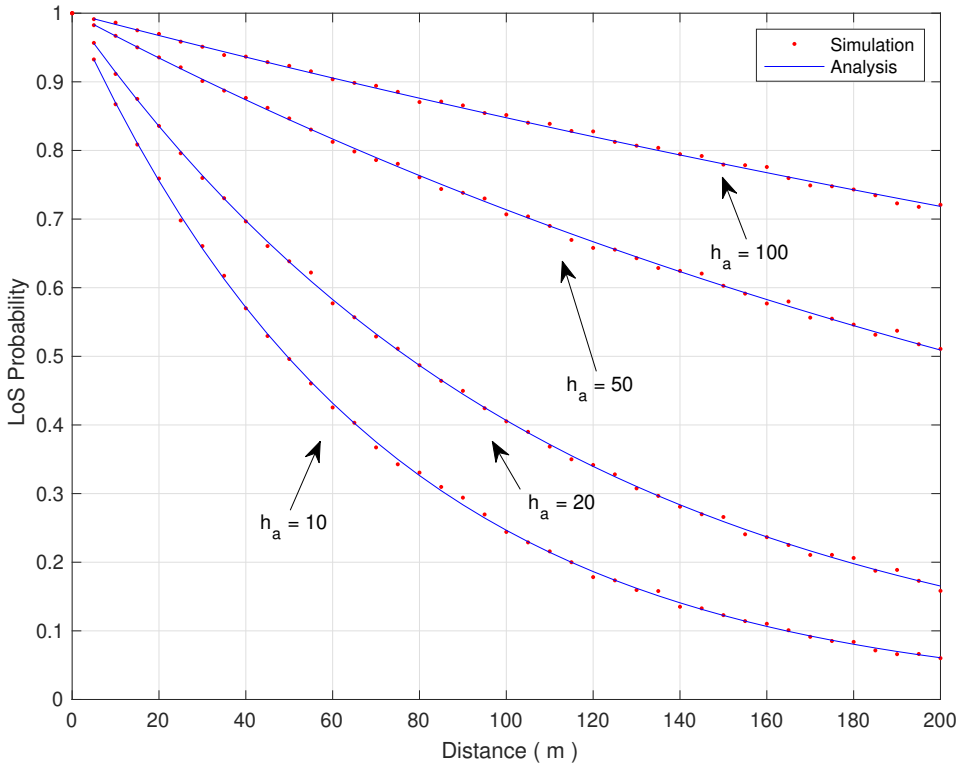

Figure 2.3: Probability of obtaining LoS from a ground user located at 0 and to an UAV located at x_a for a Uniform height distribution and $h_g = 2m$. Solid lines show the numerical results calculated using our closed-form expressions, while the dots show results generated by Monte Carlo simulation.

are potentially more blockages.

2.5 Analysis of Truncated Gaussian Random Height Distributions

2.5.1 Derivation of Closed-form Expression

Consider the case that the heights of the blockages are drawn from a truncated Gaussian random variable. The truncation is required to guarantee that the height cannot be negative. The truncated Gaussian uses a Gaussian random variable with mean μ and standard deviation σ as its parent distribution, and is truncated to the range $h \geq 0$. The cdf of this

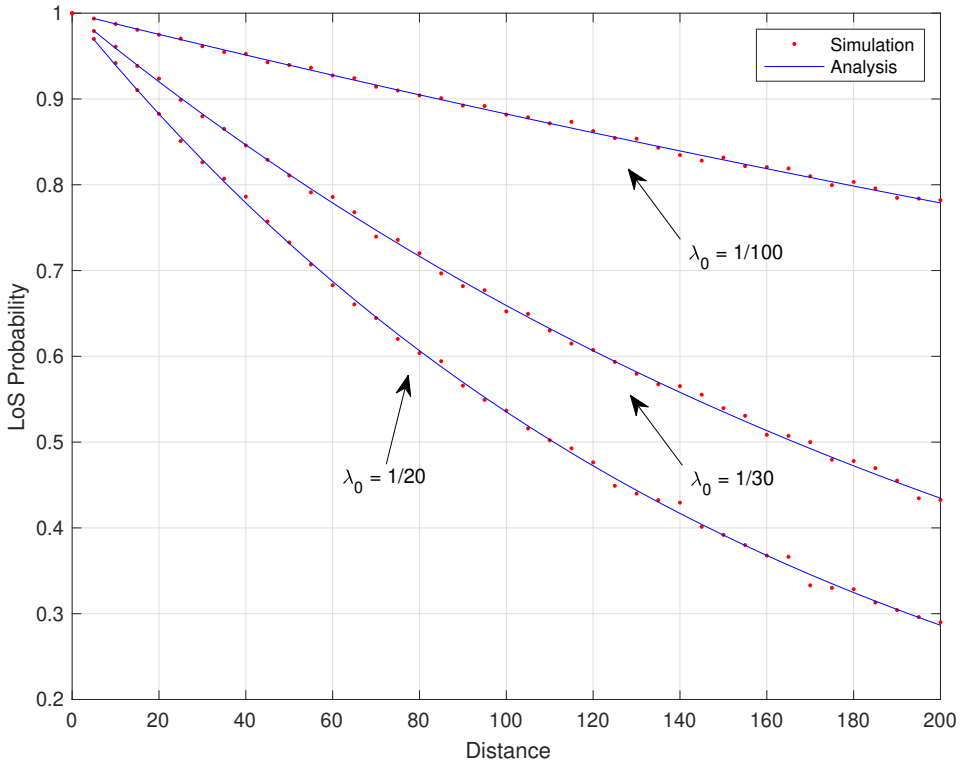

Figure 2.4: Probability of obtaining LoS from a ground user located at 0 and to an UAV located at x_a for a Uniform height distribution and $h_g = 2m$. Solid lines show the numerical results calculated using our closed-form expressions, while the dots show results generated by Monte Carlo simulation.

variable is

$$F_H(h) = \frac{Q\left(\frac{\mu - h}{\sigma}\right) - Q\left(\frac{\mu}{\sigma}\right)}{1 - Q\left(\frac{\mu}{\sigma}\right)}, \tag{2.20}$$

for $h \geq 0$, and zero elsewhere, where $Q(\cdot)$ is the Q-function.

For the truncated Gaussian distribution, the density of the inhomogenous PPP is given by (2.8), where $F_H(\cdot)$ is given by (2.20) and $h_c(\cdot)$ is given in (2.5).

The resulting density is

$$\lambda(x) = \lambda_0 \left(\frac{\Phi\left(\frac{\mu - h_c(x)}{\sigma}\right)}{\Phi\left(\frac{\mu}{\sigma}\right)} \right). \tag{2.21}$$

where

$$\Phi(z) \quad = \quad 1 - Q(z) = \frac{1}{2}\left(1 + \text{erf}\frac{z}{\sqrt{2}}\right) \tag{2.22}$$

is the cdf of the standard normal distribution.

The integral in (2.9) is

$$\int_0^{x_a} \lambda(x)dx = \frac{\lambda_0}{\Phi\left(\frac{\mu}{\sigma}\right)} \int_0^{x_a} \Phi\left(\frac{\mu - h_c(x)}{\sigma}\right) dx. \tag{2.23}$$

From (2.22), this can be rewritten as

$$\begin{aligned} \int_0^{x_a} \lambda(x)dx &= c \int_0^{x_a} \left(1 + \text{erf}(a - bx)\right) dx \\ &= c\left(x_a + \int_0^{x_a} \text{erf}(a - bx)\right) dx \end{aligned} \tag{2.24}$$

Where we can substitute the following with

$$a = \frac{(\mu - h_g)}{(\sqrt{2}\sigma)} \tag{2.25}$$

$$b = (h_a - h_g)(\sqrt{2}\sigma x_a) \tag{2.26}$$

$$c = \frac{\lambda_0}{2\phi\left(\frac{\mu}{\sigma}\right)} \tag{2.27}$$

The integral on the second line of (2.24) can be found in closed form from mathematical handbooks (e.g. [25]) to be

$$\frac{e^{-a^2} + \sqrt{\pi}\left[(bx_a - a)\text{erf}(a - bx_a) + a\text{erf}(a)\right] - e^{-(a-bx_a)^2}}{\sqrt{\pi}b}. \tag{2.28}$$

The LoS probability is then found by substituting (2.24) into (2.9)

$$\mathbb{P}_{LoS}^{ga}(x) = \exp\left(-c\left[x_a + \left(\int_0^{x_a} \text{erf}(a - bx)dx\right)\right]\right) \tag{2.29}$$

Now we can solve the integral with the closed form equation found in (2.28)

$$\mathbb{P}_{LoS}^{ga}(x) = \exp\left(-c\left[x_a + \frac{e^{-a^2} + \sqrt{\pi}\left[(bx_a - a)\text{erf}(a - bx_a) + a\text{erf}(a)\right] - e^{-(a-bx_a)^2}}{\sqrt{\pi}b}\right]\right) \tag{2.30}$$

2.5.2 Simulation and Analysis Validation

In this section, we present numerical results generated by our methods. The key part of these methods is the calculation of the probability of obtaining a LoS between the ground user and the UAV. We consider a Poisson forest where the locations of the blockages along a straight line are generated via a Poisson point process. The distributions of the blockages height H_t were chosen to be a Truncated Gaussian distribution with cdf $F_H(h)$ defined as in (2.21)

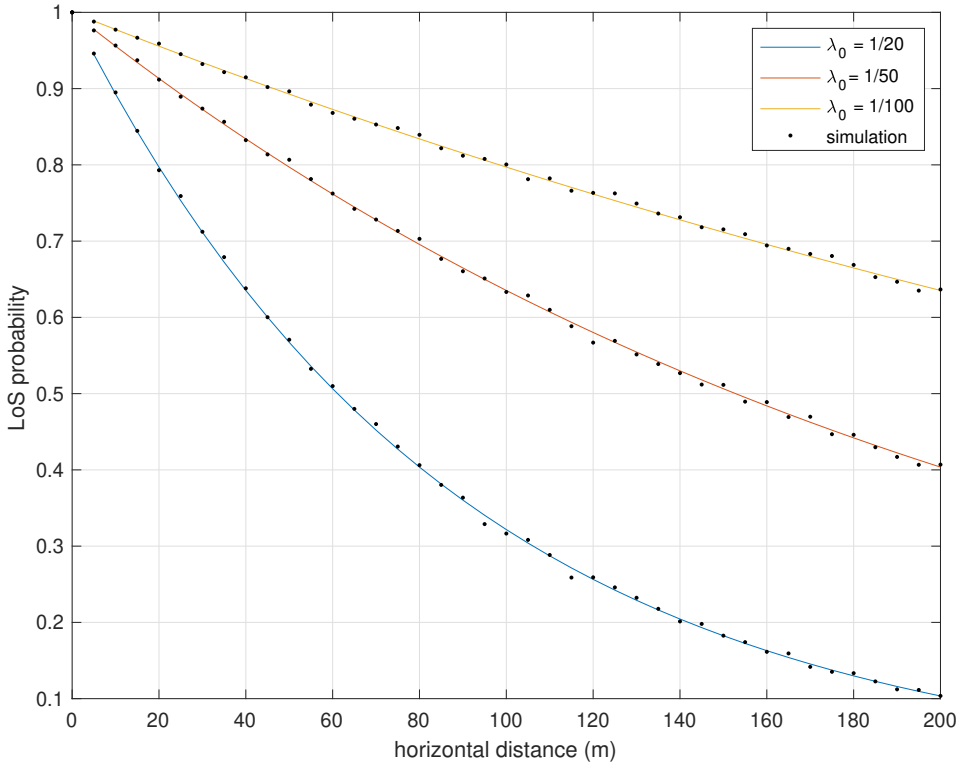

Figure 2.5: Probability of obtaining LoS from a ground user located at 0 and to an UAV located at x_a for a truncated Gaussian height distribution and $h_g = 2m$. Solid lines show the numerical results calculated using our closed-form expressions, while the dots show results generated by Monte Carlo simulation.

The simulation validated our numerical findings using the same methodology as for the Uniform distribution, with the exception that the heights are drawn from a truncated Gaussian distribution.

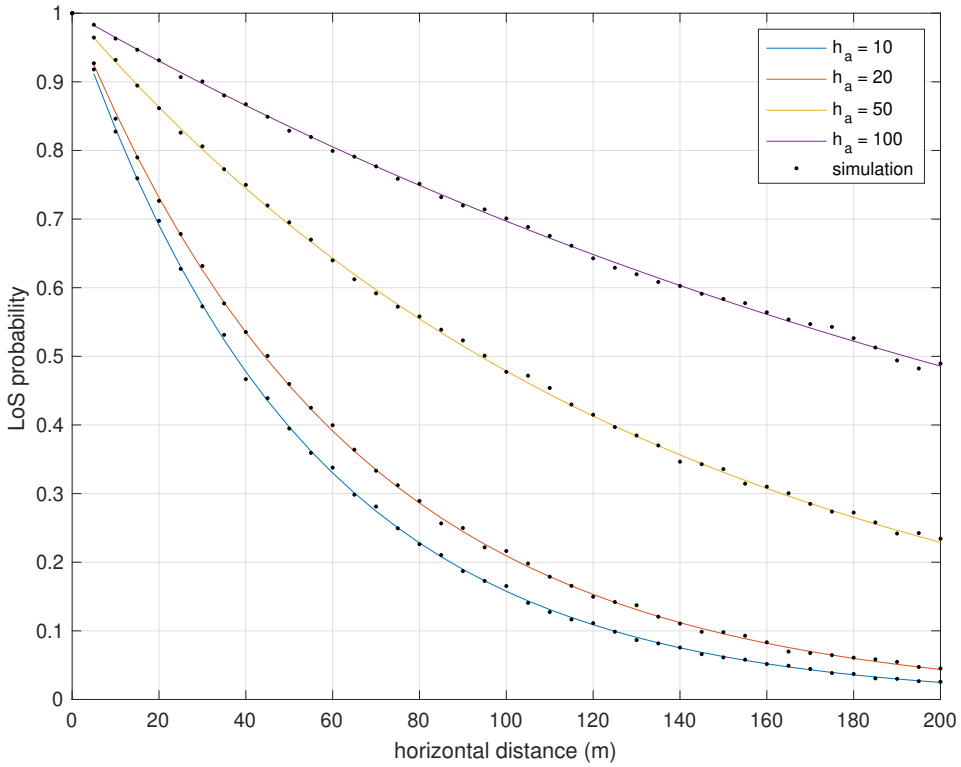

Figure 2.6: Probability of obtaining LoS from a ground user located at 0 and to an UAV located at x_a for a truncated Gaussian height distribution and $h_g = 2m$. Solid lines show the numerical results calculated using our closed-form expressions, while the dots show results generated by Monte Carlo simulation.

Figure 2.5 shows the probability of obtaining LoS between a ground user and UAV, $\mathbb{P}LoS^{ga}(x)$, with the horizontal distance x_a. In this figure we parameterized over different density λ_0. The UAV flies with the altitudes of $h_a = 80$ meters. The ground user has a communication device fixed at the height of $h_g = 2$. The results shows that $\mathbb{P}^{ga}_{LoS}(x)$ decreases as λ_0 increases since there are more blockages.

Figure 2.6 shows the probability of obtaining LoS between a ground user and UAV, $\mathbb{P}LoS^{ga}(x)$, with the horizontal distance x_a. In this figure we parameterized over different UAV heights h_a. The UAV flies with different heights of $h_a = [10, 20, 50, 100]$ meters. The ground user has a communication device fixed at the height of $h_g = 2$. The results shows that $\mathbb{P}^{ga}_{LoS}(x)$ increases as h_a increases. The reason behind it is that as the h_a increases it will be potentially be higher than the critical height which leads to obtaining the LoS.

2.6 Chapter Summary

The methodology introduced in this chapter can compute the LoS probability for a fixed single UAV in a one dimensional network. The probability is found by finding the void probability of an inhomogenous PPP, whose intensity is a function of distance due to a critical-height function that is also a function of distance but can be found through linear interpolation. The application covered in this chapter is therefore not exclusive to a certain form of distribution for the height of the blockages. Consequently, we have been able to establish closed form equations for both cases. Uniform and the truncated Gaussian distributions. Simulation results validate the theoretical expression.

Chapter 3

Relaying Through a UAV At Fixed Location

3.1 System Model

Consider a network consisting of two ground assets with a height of h_g located along the horizontal coordinate, where the first ground asset is located at $x = 0$, and the second ground asset is located at x_g.The blockages are drawn from a one-dimensional PPP of density λ_0. The air asset at an altitude of h_a is available to aid in the communication, for instance, by receiving the signal transmitted to it by the first ground asset and relaying it to the second ground asset. We limit the horizontal location of the air asset to be along the straight line $(0, x_g)$ that connects the two ground assets. If we define x_a to be the horizontal location of the air asset, then $0 \leq x_a \leq x_g$ as shown in figure 3.1.

3.2 Obtaining LoS Probability

3.2.1 LoS of (Ground-to-Ground) Assets

Two ground assets with heights of h_g located along the horizontal distance $(0, x_g)$. Only blockages that are taller than h_g cause an obstruction and block the view between the pair of ground assets. In order to obtain the LoS, we need to set the critical height of the blockages $h_c = h_g$. Since h_c is a constant the blockages are described as homogeneous PPP. Therefore,

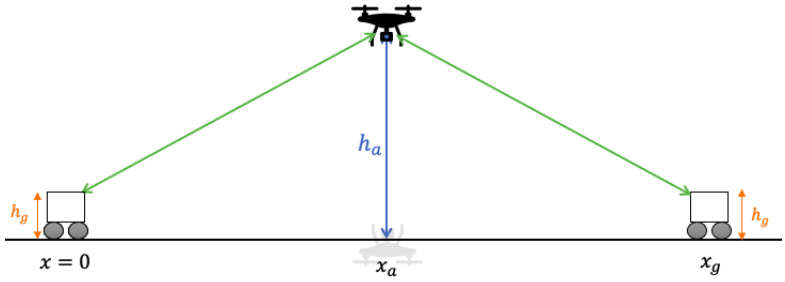

Figure 3.1: Example of one dimensional aerial network consisting of two ground assets with a height of h_g. The first asset is located at $x = 0$ and the second ground asset is located at x_g along the horizontal coordinate. In addition, a UAV flies at an altitude of h_a denoted by the blue line, where the shadow of the UAV is located at x_a. The left green link denotes a LoS link between the ground asset-to-UAV .The right green link denotes a LoS link from UAV-to-ground asset.

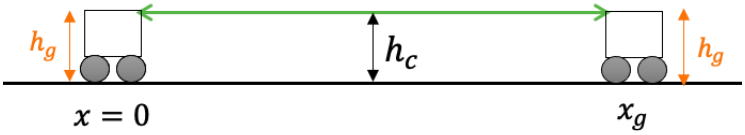

Figure 3.2: Example of one dimensional aerial network consisting of two ground assets with a height of h_g. The first asset is located at $x = 0$ and the second ground asset is located at x_g along the horizontal coordinate. The green link denotes a LoS link between the two ground assets.

the probability of obtaining the LoS of two ground assets is the void probability of the homogeneous PPP of density

$$\lambda_c = \lambda_0 \left[1 - F_H(h_c)\right] \tag{3.1}$$

Over an interval of length x_g. The probability of LoS of two ground assets is found by

$$\mathbb{P}_{LoS}^{gg} = e^{-\lambda_0[1-F_H(h_g)]x_g} \tag{3.2}$$

3.2.2 LoS of (Ground-to-Air-Ground) Assets

In order to obtain the LoS Probability of air-assisted communications, we will need to consider the communication of ground-air-ground (i.e., air-aided) connections as two hops or two links. Where $\mathbb{P}_{LoS}^{ga}$ and $\mathbb{P}_{LoS}^{ag}$ is the LoS probabilities of the ground-to-air and air-to-

ground links. In chapter 2, we have discussed the method of obtaining the LoS probability for the ground-to-air link by deriving the closed form expression for $\mathbb{P}_{LoS}^{\mathsf{ga}}$. We can obtain the probability of air-to-ground link $\mathbb{P}_{LoS}^{\mathsf{ag}}$ using a similar analysis. As mentioned, we are considering the communication as two separate links. However, each link is independent of the other. Therefore, to obtain end-to-end communication we need to find the LoS probability of ground-air-ground link $\mathbb{P}_{LoS}^{\mathsf{gag}}$

$$\mathbb{P}_{LoS}^{\mathsf{gag}} = \mathbb{P}_{LoS}^{\mathsf{ga}} \mathbb{P}_{LoS}^{\mathsf{ag}} \tag{3.3}$$

3.3 Throughput

While the LoS probability is useful for predicting the existence of a LoS between two assets, it does not characterize the *quality* of the link, which is also affected by the transmission distance of each link. For instance, if one wants to determine the height of an air asset that maximizes *only* the end-to-end LoS probability with a ground asset, the solution would be to place the air asset at an infinite height so that the critical heights at any location between the two assets are infinite (*i.e.*, no blockage is able to obstruct the unblocked view between them). Such solution is neither practical nor efficient in reality due to the significant signal loss caused by the infinite transmission distance.

An appropriate metric that captures the loss of signal power at distance is the expected *throughput*, which we here define to be the maximum achievable data rate when accounting for the possibility of blockage. For a single hop, the expected throughput is

$$T = \mathbb{P}_{LoS} C, \tag{3.4}$$

where C is the *capacity* of the link, and the multiplication by $\mathbb{P}_{LoS}$ accounts for the expectation being with respect to LoS. Here, we set C as the Shannon Capacity, which is the maximum achievable rate of an unblocked link

$$C = B \log_2 (1 + \mathsf{SNR}), \tag{3.5}$$

where B is the signal bandwidth, and the signal-to-noise ratio, when expressed in dB, is

$$\mathsf{SNR}^{\mathsf{dB}} = \mathsf{SNR}_0^{\mathsf{dB}} - 10\alpha \log_{10}\left(\frac{d}{d_0}\right), \tag{3.6}$$

where α is the path-loss exponent, d_0 is a reference distance typically set to 1 meter, and $\mathsf{SNR}_0^{\mathsf{dB}}$ is the SNR when the receiver is placed at distance d_0 assuming free-space propagation up to that distance. The value of $\mathsf{SNR}_0^{\mathsf{dB}}$ can be measured, or it can be calculated from the transmit power, carrier frequency, bandwidth, receiver's noise figure, and antenna gains.

For a direct ground-ground transmission, the expected throughput is computed from (3.4) with d in (3.6) set to x_g. For a two-hop ground-air-ground transmission, it depends on the LoS probabilities of both hops. As stated previously, $\mathbb{P}_{LoS}^{\mathsf{ga}}$ and $\mathbb{P}_{LoS}^{\mathsf{ag}}$ are LoS probabilities of the ground-to-air and air-to-ground links, respectively, and similarly define C_{ga} and C_{ag} as the two capacities, the expected throughput for the ground-air-ground communication is

$$T = \frac{1}{2}\mathbb{P}_{LoS}^{\mathsf{ga}}\mathbb{P}_{LoS}^{\mathsf{ag}} \min(C_{\mathsf{ga}}, C_{\mathsf{ag}}), \tag{3.7}$$

where the multiplication by $1/2$ accounts for the time-division duplexing (TDD) operation at the air asset (*i.e.*, the air asset spends half its time receiving from the first ground asset and half its time transmitting to the second ground asset). Alternatively, frequency-division duplexing (FDD) can be used, but in that case, the per-link capacities should be scaled accordingly since only half of the band could be used for each hop. Each capacity is found from (3.5) with the distance in (3.6) set as the Euclidean distance between the air antenna and the corresponding ground antenna, where each distance is the hypotenuse of a right triangle formed with one leg being the horizontal distance, either x_a for the ground-air link or $x_g - x_a$ for the air-ground link, and the other leg being the difference in antenna heights, $h_a - h_g$. Notice that the ground-air-ground throughput is determined by the minimum capacity of the two hops, which motivates us to consider deploying the aiding air asset always above the midpoint of the two ground assets.

3.4 Simulation

We performed Monte Carlo simulations involving the repeated drawing of Poisson forests. Let ℓ be the interval of a simulated Poisson forest, where $\ell = x_g$ for a ground-ground link

or $\ell = x_a$ for a ground-air link. Drawing a Poisson forest involves first determining the random number N of obstructions in the interval, which is done by drawing N from a Poisson distribution of mean $\lambda_0 \ell$. Next, each of the N obstructions is placed uniformly over the interval. Then, each blockage's height is determined by randomly drawing its H from the corresponding distribution. Once the forest was constructed, it was determined whether or not the LoS path was blocked by checking to see if any of the obstructions were above the critical height at that location. This process was repeated for 500 thousand trials for each data point reported.

We compare the end-to-end LoS probability $\mathbb{P}_{LoS}$ of direct ground-ground communication with air-aided ground-air-ground communication. When making this comparison, the air asset is always deployed above the midpoint of the two ground assets; i.e., $x_a = x_g/2$. In this scenario, the probability to obtain LoS from the air asset to both ground assets synchronously is the square of $\mathbb{P}^{ga}_{LoS}$. We assume that the air asset is flying at a height of $h_a = 100$ m, while all ground assets have their communication devices fixed at a height of $h_g = 2$ m. Both the truncated Gaussian and the uniform height distributions are considered.

In addition, we computed the throughput performance for the same scenarios previously discussed. The additional parameters required to compute the throughput are a reference SNR of $\mathsf{SNR}_0^{\mathsf{dB}} = 81.98$ dB at a reference distance of $d_0 = 1$ meter, a path-loss coefficient of $\alpha = 2.3$, and a bandwidth of $B = 20$ MHz. This path-loss coefficient corresponds to the one reported in [26] for the measured LoS pathloss at 38 GHz. The reference SNR is computed for a transmit power of 0 dBm, a receiver noise figure of 9 dB, and antenna gains of 12.1 dBi for both the transmit and receive antennas, which are the gains reported for a compact 6-element array operating at 38 GHz in [27]. We consider the same obstacle models as before, with $\lambda = 0.02$ and height distributions that are either a truncated Gaussian (with $\mu = 19$ and $\sigma = 10$) or a uniform (with $h_{max} = 29$). The ground asset's antenna height is set to $h_g = 2$ m.

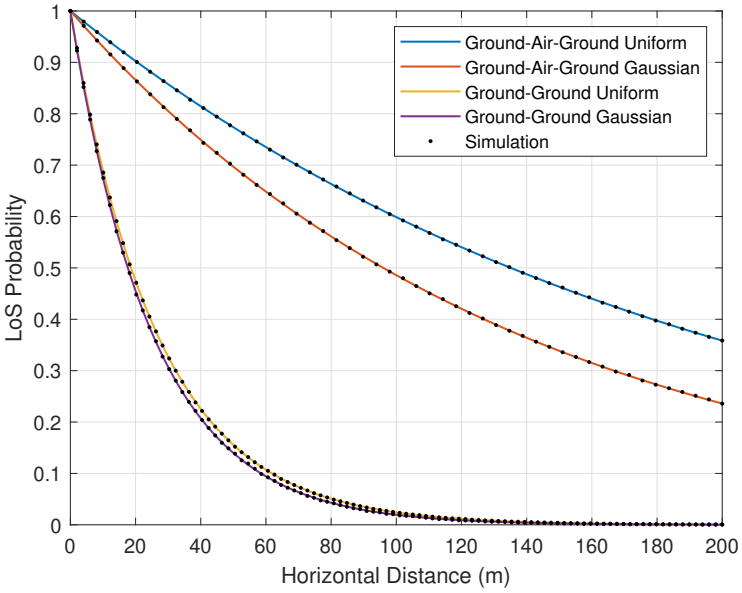

Figure 3.3: Probabilities of obtaining the LoS for ground-air-ground and ground-ground communication for $h_a = 100$ m and $h_g = 2$ m. Solid lines show the numerical results calculated using our closed-form expressions, while the dots show results generated by Monte Carlo simulation.

Figure 3.3 shows the results of this comparison. For direct ground-ground communication, the probability of obtaining LoS decreases much faster as a function of distance than in the case of air-aided ground-air-ground communication. For the truncated Gaussian distribution, when $\mu = 19$ m and $\sigma = 10$ m, (2.20) suggests that most of the blockages will be taller than 2 m. Thus, almost all blockages can obstruct the unblocked view between a pair of ground assets, severely decreasing the probability of obtaining the LoS. For the uniform distribution, according to (2.10), there is a probability greater than 0.92 that the heights of the blockages are taller than h_g. This causes a fast decrease in the $\mathbb{P}_{LoS}$ for the ground-ground communication, which is similar to what is observed for the truncated Gaussian distribution.

When $x_a = 60$ m, i.e., the probability of obtaining LoS between ground assets using direct ground-ground communication is approximately 0.1 for both the truncated Gaussian and the uniform distributions. However, when an air asset is used, the probability that it obtains a LoS with both ground assets is approximately 6.5 and 7.3 times greater than the probability of the two ground assets obtaining LoS over a direct link considering the truncated Gaussian and uniform distributions, respectively.

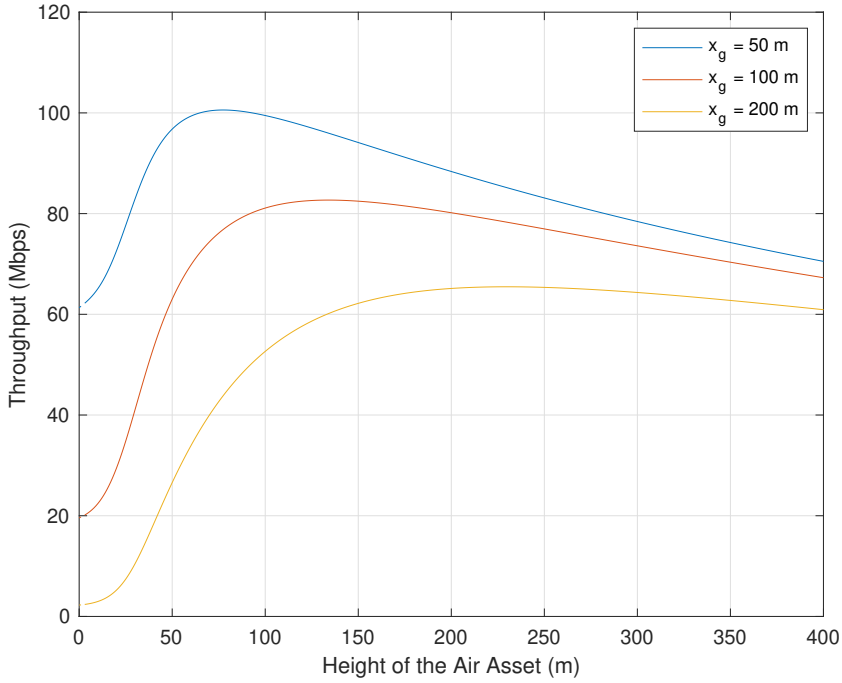

Figure 3.4: Throughput of ground-air-ground communication as a function of the height h_a of the air asset for horizontal distances $x_g = \{50, 100, 200\}$ m considering a Gaussian truncated distribution and $h_g = 2$ m.

Figure 3.3 shows that the choice of distribution does not have a significant impact on the probability of obtaining the LoS between ground assets using the direct link, since the communication devices of the ground assets are fixed at a relatively low height and therefore the LoS would be easily obstructed by most blockages. On the other hand, when an air asset is used, the height distribution has a bigger impact on the LoS probability since the differences of the distributions become more pronounced.

Figure 3.4 shows throughput as a function of the height of the air asset, h_a, for several different distances between ground assets, x_g. The air asset is located at the midpoint between the two ground assets, i.e. $x_a = x_g/2$, and this figure shows results for just the truncated Gaussian height distribution (results for the uniform distribution are similar). As expected, the throughput is higher when the ground assets are closer to each other. However, for each curve, a peak value can be observed. Lowering the altitude of the air asset below this peak makes it prone to blocking, but raising it above the peak value causes a loss in signal

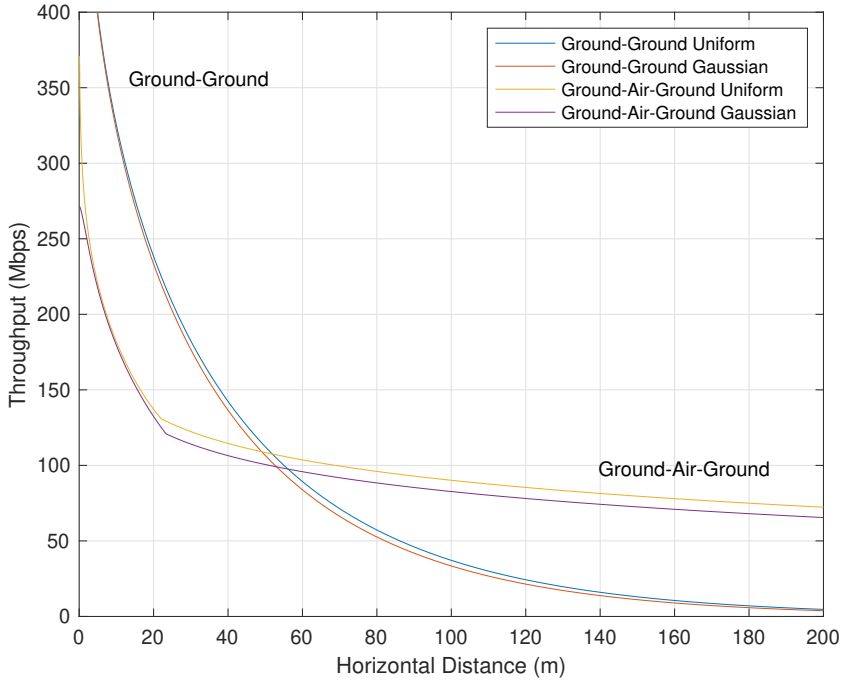

Figure 3.5: Throughput as a function of horizontal distance x_g for both truncated Gaussian and uniform height distributions. Results are shown for direct ground-ground communication as well as for relayed ground-air-ground communication. In the case of ground-air-ground communication, the throughput is optimized with respect to the height h_a of the air asset.

power which translates to a loss of capacity. The peak value balances the assets' capability of obtaining LoS and the signal power, which is a key tradeoff as both contribute to the throughput. For x_g equal to 50 m, 100 m, and 200 m, the peak values are 100.6 Mbps, 82.7 Mbps, and 65.5 Mbps, respectively, and these peaks occur at h_a of 77 m, 134 m, and 230 m, respectively.

Figure 3.5 shows throughput as a function of the horizontal distance x_g between the ground assets. The figure shows results for both truncated Gaussian and uniform height distributions and for both direct ground-ground communication and relayed ground-air-ground communication. For ground-air-ground communication, the throughput is optimized at each distance by maximizing its value over the height of the air asset h_a. For direct ground-ground communication, no such optimization is possible. The plot shows that, for sufficiently far distances, the throughput of the ground-air-ground communication is higher than that of the direct ground-ground communication. However, for shorter distances, ground-ground com-

munication has a higher throughput. When the height distribution is a truncated Gaussian, this crossover occurs at a distance of $x_g = 52.9$ m, where the throughput for both direct ground-ground and relayed ground-air-ground communications is 99 Mbps. The reason that direct ground-ground communications performs better at ranges closer than this crossover distance is primarily due to the need for the air asset to duplex the signal received from the first ground asset and transmitted to the second ground asset. The direct link does not need to duplex. However, at longer distances, maintaining a direct link between the two ground assets suffers from a lower probability of obtaining a LoS and a weaker signal power due to the long single transmission path.

3.5 Chapter Summary

In this chapter, we have extended our ability to obtain LoS probability using the closed form analysis found in chapter 2 for Uniform and Truncated Gaussian height distribution. In this chapter, we were able to explore the LoS link between a pair of ground assets. In addition, we have also examine the probability of LoS with respect to end-to-end communication when the communication is air assisted. Finally, we have also establish *throughput* as a metric that balances communication distance with the impact of LoS blockage. Throughput is used to determine the range at which it is better to relay communications through the air asset, and, when the air asset is deployed, its optimal height.

Chapter 4

Analysis with a Randomly Located UAV

4.1 System Model

Again consider a network with a ground user located at $x = 0$, a single UAV, and randomly located potential blockages (*i.e.*, buildings, trees) of a non-trivial thickness. Once again the potential blockages are drawn from a one-dimensional homogeneous PPP of density λ_0. The number of potential blockages along the horizontal coordinate from the the ground user to the shadow of the UAV is equal to N, where N is a Poisson random variable. The locations of each blockage $B_k, k \in \{1, ...N\}$ are uniformly distributed, and their heights H_k are assumed to be uniformly distributed in this chapter. As stated in Chapter 2, we assume that the heights of the N blockages are independent and identically distributed (i.i.d.) and that their cumulative distribution function (cdf) is $F_H(h)$. Whereas in the previous chapters, we have placed the UAV at a fixed (deterministic) location, in this chapter the UAV is now deployed randomly along the horizontal coordinate x while the altitude h_a remains fixed. Hence, the horizontal distance to the UAV x_a is now a random variable x_a as shown in 4.1. This chapter focuses on how to statistically characterize the LoS probability when the distance x_a is random.

As shown in Chapter 2, the LoS probability is a function of the distance x_a along the ground plane. For instance, Fig. 2.2 shows that as the UAV gets further away, i.e., x_a

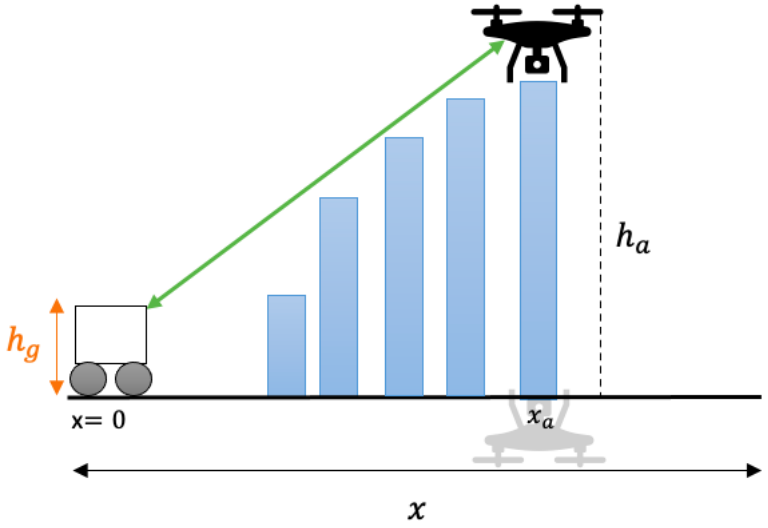

Figure 4.1: Example of one dimensional aerial network consisting of a UAV, a ground user with antenna height h_g, and randomly located potential blockages. The blue bars show example potential blockages that are all below the critical height shown by the green line that connects the ground user to the UAV. The black dashed line indicates the height of the UAV. The gray shadow of the UAV demonstrates to the UAV location along the horizontal distance, and here this distance is a random variable x_a.

increases, the LoS probability gets smaller. This intuitively makes sense, since at further distances, the elevation angle from the ground user to the UAV decreases, lowering the critical height at close range and therefore making it easier for a potential blockage to be high enough to become an actual blockage. When x_a is random, then the LoS probability expressions found in Chapter 2 can be interpreted as a *function* of a random variable since the LoS probability depends on x_a. Under this viewpoint, the LoS probability is itself a random variable, since any function of a random variable is also a random variable. Thus, the key concept in the analysis presented below is to interpret the LoS probability as a random variable, where the randomness is due to the randomness of x_a. Like any random variable, this random variable can be characterized by its cumulative distribution function, which is found in the analysis.

4.2 Uniform Distribution

4.2.1 Analysis of a Uniform Distribution

In Chapter 2, we derived a closed-form expression of $\mathbb{P}_{LoS}^{ga}$, which is the LoS probability from the ground user to the UAV, for two height distributions, including a uniform height distribution. Whereas that analysis assumed a fix location for the UAV, in this chapter we allow the horizontal distance x_a to be random. Accordingly, the analysis of $\mathbb{P}_{LoS}^{ga}$ must be extended, as discussed below.

The starting point for this analysis is equation (2.19), which is the final closed-form expression for $\mathbb{P}_{LoS}^{ga}$ with a uniform height distribution. This equation involves two cases, with the first case for when $x_a > x_c$ and the second case for when $x_a \leq x_c$. Recall that x_c, as defined at (2.13), is the critical distance such that any potential blockage located at $x > x_c$ and cannot block the LoS because at those locations, $h_c(x) > h_{max}$.

Under the assumption that x_a is uniformly distributed between $(0, X)$, where X represents the maximum distance, the cdf of x_a is $F_{x_a}(z) = \mathbb{P}[X \leq z]$ given by:

$$F_{x_a}(z) = \begin{cases} \dfrac{z}{X} & \text{for } 0 \leq z \leq X \\ \\ 1 & \text{for } z > X \end{cases} \tag{4.1}$$

The pdf of $f_{x_a}(z)$

$$f_{x_a}(z) = \begin{cases} \dfrac{1}{X} & \text{for } 0 \leq z \leq X \\ \\ 0 & \text{for otherwise} \end{cases} \tag{4.2}$$

Now, from Chapter 2, we know that the LoS Probability is a function of the random variable x_a. Hence, the LoS Probability is in itself a probability, since it is a function of a random variable. This functional dependence can be explicitly shown by expressing the LoS Probability as $\mathbb{P}_{LoS}(x_a)$. As a random variable, we wish to characterize the LoS Probability by its cdf, defined as the probability that it is below some threshold, i.e.,

$$F_{\mathbb{P}_{LoS}}(z) = \mathbb{P}\left[\mathbb{P}_{LoS}(x_a) \leq z\right] \tag{4.3}$$

First consider the case that $x_c \geq x_a$, in which case $\min(x_a, x_c) = x_a$ in (2.19), and thus the LoS Probability is given by:

$$\mathbb{P}_{LoS}(x_a) = e^{-\lambda_0 x_a \left[1 - \frac{h_g}{h_{\max}} - \left(\frac{h_a - h_g}{2 x_a h_{\max}}\right) x_a\right]}$$

Simplifying LoS probability equation

$$\mathbb{P}_{LoS}(x_a) = e^{\frac{\lambda_0 x_a (h_g - 2h_{max} + h_a)}{2h_{max}}} \tag{4.4}$$

Substituting the above equation into (4.3) gives the cdf:

$$F_{\mathbb{P}_{LoS}}(z) = \mathbb{P}\left[e^{\frac{\lambda_0 x_a (h_g - 2h_{max} + h_a)}{2h_{max}}} \leq z\right] \tag{4.5}$$

We want to solve for the random location of the UAV which is denoted by x_a.The functional transformation is as follows

$$F_{\mathbb{P}_{LoS}}(z) = \mathbb{P}\left[x_a \leq \frac{\ln z^2 h_{max}}{\lambda_0 (h_g - 2h_{max} + h_a)}\right] \tag{4.6}$$

Lets call the right hand side fraction γ_1.

$$\gamma_1 = \frac{2 \ln z h_{max}}{\lambda_0 (h_g - 2h_{max} + h_a)} \tag{4.7}$$

Evaluating the cdf of $\mathbb{P}_{LoS}(x_a)$

$$F_{\mathbb{P}_{LoS}(x_a)} = \int_{\gamma_1}^{X} \frac{1}{X} dx_a \tag{4.8}$$

$$F_{\mathbb{P}_{LoS}(x_a)} = 1 - \frac{\gamma_1}{X} \tag{4.9}$$

Therefore, our $F_{\mathbb{P}_{LoS}(x_a)}(z)$ will be

$$F_{\mathbb{P}_{LoS}(x_a)}(z) = \begin{cases} 1 - \dfrac{\gamma_1}{X} & \text{for } z \leq e^{\frac{X \lambda_0 (h_g - 2h_{max} + h_a)}{2h_{max}}} \\ \\ 0 & \text{for otherwise} \end{cases} \tag{4.10}$$

if $x_a > x_c$, where we just have substitute in the equation of x_c in (2.19) instead of $\min(x_a, x_c)$. So our new $\mathbb{P}_{LoS}(x_a)$

$$\mathbb{P}_{LoS}(x_a) = e^{-\lambda_0 x_c \left[1 - \frac{h_g}{h_{\max}} - \left(\frac{h_a - h_g}{2x_a h_{\max}}\right) x_c\right]}. \tag{4.11}$$

Now plug in the equation of x_c

$$\mathbb{P}_{LoS}(x_a) = e^{-\lambda_0 \left(\frac{h_{\max} - h_g}{h_a - h_g}\right) x_a \left[1 - \frac{h_g}{h_{\max}} - \left(\frac{h_a - h_g}{2x_a h_{\max}}\right) \left(\frac{h_{\max} - h_g}{h_a - h_g}\right) x_a\right]} \tag{4.12}$$

Simplifying the equation we can obtain final equation $\mathbb{P}_{LoS}(x_a)$

$$\mathbb{P}_{LoS}(x_a) = e^{-\frac{\lambda_0 x_a (h_{max} - h_g)^2}{2h_{max}(h_a - h_g)}} \tag{4.13}$$

As stated earlier now we have our $\mathbb{P}_{LoS}(x_a)$ equation as a function of random variable therefore,for this case we can find the cdf of the function of random variable $F_{\mathbb{P}_{LoS}}(z) = \mathbb{P}\left[\mathbb{P}_{LoS}(x_a) \leq z\right]$. The functional transformation is as follows

$$F_{\mathbb{P}_{LoS}}(z) = \mathbb{P}\left[e^{\frac{-\lambda_0 x_a (h_{max} - h_g)^2}{2h_{max}(h_a - h_g)}} \leq z\right] \tag{4.14}$$

We want to solve for the random location of the UAV which is denoted by x_a

$$F_{\mathbb{P}_{LoS}}(z) = \mathbb{P}\left[x_a \geq \frac{-2 \ln z h_{max}(h_a - h_g)}{\lambda_0 (h_{max} - h_g)^2}\right] \tag{4.15}$$

Lets call the right hand side fraction γ_2.

$$\gamma_2 = \frac{-2 \ln z h_{max}(h_a - h_g)}{\lambda_0 (h_{max} - h_g)^2} \tag{4.16}$$

Evaluating the integral of $F_{\mathbb{P}_{LoS}}(x_a)$

$$F_{\mathbb{P}_{LoS}(x_a)} = \int_{\gamma_2}^{X} \frac{1}{X} dx_a \tag{4.17}$$

$$F_{\mathbb{P}_{LoS}(x_a)} = 1 - \frac{\gamma_2}{X} \tag{4.18}$$

Therefore, our $F_{\mathbb{P}_{LoS}}(z)$ will be

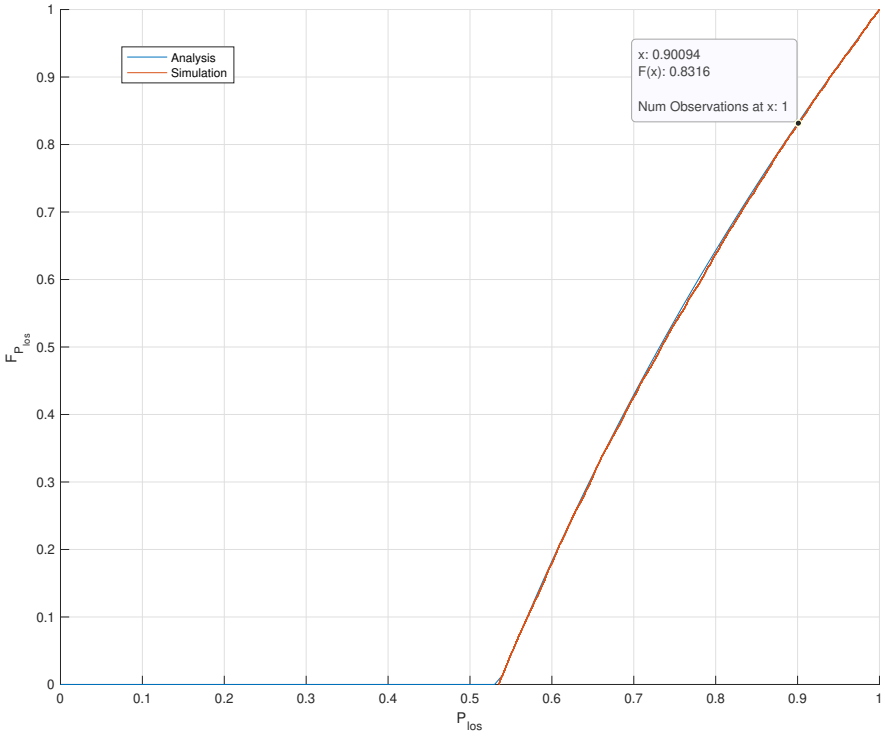

Figure 4.2: The empirical cumulative distribution function (CDF) of $\mathbb{P}_{LoS}$ over 10000 trial network realization

$$F_{\mathbb{P}_{LoS}}(z) = \begin{cases} 1 - \dfrac{\gamma_2}{X} & \text{for } z \geq e^{\frac{-X\lambda_0(h_{max}-h_g)^2}{2h_{max}(h_a-h_g)}} \\ \\ 0 & \text{for otherwise} \end{cases} \tag{4.19}$$

4.2.2 Simulation and Validations

To validate the numerical results without loss of generality we assumed the user have no significant height $h_g = 0$. During each trial, the UAV will have a new random location each time. Given that random location of the UAV, we compute the Los probability using our analysis found in (4.10) and store it in a vector. Where the vector will contain a set of randomly generated LoS probability that will help show the empirical cdf of the LoS Probability. That is because our LoS probability is now a function of random variable. This process was repeated for 10 thousand trials for each data point reported.

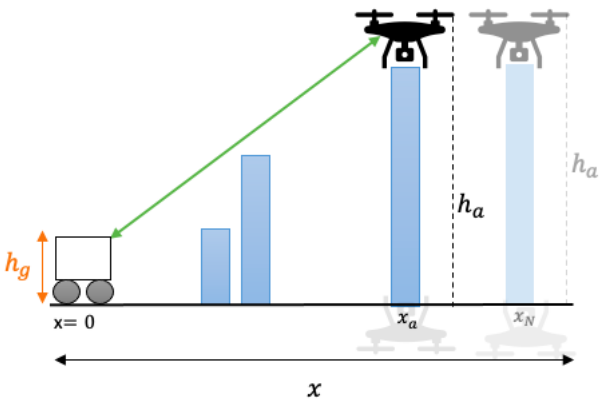

Figure 4.3: Example of one dimensional aerial network consisting of UAV, ground user and blockages with no trivial thickness. The blue bars denotes to the random blockages with critical heights. Green line indicates LoS link from the ground user to the UAV.The black dashed line indicates the height of the UAV. However, the gray shadow of the UAV demonstrates to the UAV location along the horizontal distance.

Figure (4.2) shows obtaining the LoS probability against the empirical cdf of LoS probability as a function of random variable depends on the distance X. The density of the blockages is $\lambda_0 = 1/20$. The blockages have a maximum height of $h_{max} = 20$ (m) with LoS. The UAV is deployed randomly over the random distance of $X = 100$ (m) with a fixed altitude of $h_a = 80$ (m). As shown in figure (4.2) the user may connect to the UAV only if $\mathbb{P}_{loS}(x) > 0.5$. Moreover, we can say that for ninety percent of the time our LoS probability is 0.8316 as shown.

Also, there are two curves plotted, the blue curve represents our analysis. One the other hand, the red curve represents our simulation. As shown in (4.2) we were able to successfully validate our analysis with simulation.

4.3 Exponential Distribution

4.3.1 Analysis of an Exponential Distribution

As was previously established, the LoS probability is also a random variable since it is a function of a random variable. As a result, the fundamental idea behind the analysis given follows is to see the LoS probability as a random variable, with the randomness occurring

from the randomness of x_a. Like any random variable, this random variable can be characterized by its cumulative distribution function, which is found in the analysis. However, the assumption is that the UAV is exponentially distributed with mean of λ_a.

if $x_c \geq x_a$. we can use the LoS probability equation found in (4.4) and apply it in respect to the new assumption made for x_a. Let X denote the maximum distance the UAV is located within that distance.

$$\mathbb{P}_{LoS}(x_a) = \begin{cases} e^{-\frac{\lambda_0 x_a (h_g - 2h_{max} + ha)}{2h_{max}}} & \text{for } x_a \leq X \\ \\ 0 & \text{for } x_a > X \end{cases} \tag{4.20}$$

The cdf of the exponential LoS probability in (4.20) will be

$$F_{\mathbb{P}_{LoS}}(z) = \mathbb{P}\left[\mathbb{P}_{LoS}(x_a) \leq z\right] \tag{4.21}$$

Since we are handling the exponential distribution we can only handle the case for $x_a \leq X$ Where our LoS Probability was obtained in (4.4) our cdf will be as follows

$$F_{\mathbb{P}_{LoS}}(z) = \mathbb{P}\left[e^{\frac{\lambda_0 x_a (h_g - 2h_{max} + ha)}{2h_{max}}} \leq z\right] \tag{4.22}$$

Solving for the transformation function in respect to x_a

$$F_{\mathbb{P}_{LoS}}(z) = \mathbb{P}\left[x_a \leq \frac{2 \ln z h_{max}}{\lambda_0 (h_g - 2h_{max} + h_a)}\right] \tag{4.23}$$

Let denote the fraction on the right-hand side γ_1

$$\gamma_1 = \frac{2 \ln z h_{max}}{\lambda_0 (h_g - 2h_{max} + h_a)} \tag{4.24}$$

Applying the Conditional Probability to the cdf in (4.21) because we can only use the case when $x_a > X$ and x_a is a random variable

$$F_{\mathbb{P}_{LoS}}(z) = \mathbb{P}\left[e^{\frac{\lambda_0 x_a (h_g - 2h_{max} + ha)}{2h_{max}}} \leq z \mid x_a \leq X\right] \mathbb{P}\left[x_a \leq X\right] + \mathbb{P}\left[0 \leq z \mid x_a > X\right] \mathbb{P}\left[x_a > X\right] \tag{4.25}$$

We can rewrite the conditional cdf (4.25) in respect to the transformation function that was found in (4.23)

$$F_{\mathbb{P}_{LoS}}(z) = \mathbb{P}\left[x_a \geq \gamma_1 \mid x_a \leq X\right] \mathbb{P}\left[x_a \leq X\right] + 1\mathbb{P}\left[x_a > X\right] \tag{4.26}$$

Finding the probability when $\mathbb{P}[x_a \leq X]$ which is the pdf of x_a

$$\mathbb{P}[x_a \leq X] = \int_0^X \lambda_a e^{-\lambda_a y} dy \tag{4.27}$$

Solving the integral and evaluating it from 0 to X

$$\mathbb{P}[x_a \leq X] = 1 - e^{-\lambda_a X} \tag{4.28}$$

Furthermore, we can now obtain the $\mathbb{P}[x_a > X]$

$$\mathbb{P}[x_a > X] = 1 - \mathbb{P}[x_a \leq X] \tag{4.29}$$

Plugging in (4.28) to (4.29)

$$\mathbb{P}[x_a > X] = e^{-\lambda_a X} \tag{4.30}$$

Conditional Probability is calculated as

$$\mathbb{P}\left[x_a \geq \gamma_1 \mid x_a \leq X\right] = \frac{\mathbb{P}\left[x_a > \gamma_1 \cap x_a \leq X\right]}{\mathbb{P}[x_a \leq X]} \tag{4.31}$$

Solving the numerator of the conditional probability found in (4.31)

$$\mathbb{P}(x_a > \gamma_1 \cap x_a \leq X) = \mathbb{P}[\gamma \leq x_a \leq X] \tag{4.32}$$

$$\mathbb{P}(x_a > \gamma_1 \cap x_a \leq X) = \mathbb{P}[x_a \leq X] - \mathbb{P}[x_a \leq \gamma] \tag{4.33}$$

$$\mathbb{P}(x_a > \gamma_1 \cap x_a \leq X) = 1 - e^{-\lambda_a X} - (1 - e^{-\lambda_a \gamma_1}) \tag{4.34}$$

$$\mathbb{P}(x_a > \gamma_1 \cap x_a \leq X) = e^{-\lambda_a \gamma_1} - e^{-\lambda_a X} \tag{4.35}$$

Finally we can obtain (4.31) by plugging in (4.28) and (4.35) back in

$$\mathbb{P}\left[x_a \geq \gamma_1 \mid x_a \leq X\right] = \frac{e^{-\lambda_a \gamma_1} - e^{-\lambda_a X}}{1 - e^{-\lambda_a X}} \tag{4.36}$$

Now we can have cdf of the LoS Probability as function of random variable will be

$$F_{\mathbb{P}_{LoS}}(z) = \begin{cases} e^{-\lambda_a \gamma_1} & \text{for } z \leq e^{\frac{\lambda_0 x (h_g - 2h_{max} + ha)}{2h_{max}}} \\ \\ e^{-\lambda_a X} & \text{for } z > e^{\frac{\lambda_0 X (h_g - 2h_{max} + ha)}{2h_{max}}} \end{cases} \tag{4.37}$$

For the second case where if $x_c \geq x_a$. we can use the LoS probability equation found in (4.13) and apply it in respect to the new assumption made for x_a

$$\mathbb{P}_{LoS}(x_a) = \begin{cases} e^{-\frac{\lambda_0 x_a (h_{max}-h_g)^2}{2h_{max}(h_a-h_g)}} & \text{for } x_a \leq X \\ \\ 0 & \text{for } x_a > X \end{cases} \tag{4.38}$$

The cdf of the exponential LoS probability in (4.38) will be

$$F_{\mathbb{P}_{LoS}}(z) = \mathbb{P}\left[\mathbb{P}_{LoS}(x_a) \leq z\right] \tag{4.39}$$

Since we are handling the exponential distribution we can only handle the case for $x_a \leq X$ our cdf will be as follows

$$F_{\mathbb{P}_{LoS}}(z) = \mathbb{P}\left[e^{-\frac{\lambda_0 x_a (h_{max}-h_g)^2}{2h_{max}(h_a-h_g)}} \leq z\right] \tag{4.40}$$

Similar approach to the uniform distribution we will obtain the cdf and with the transformation function solving it for x_a

$$F_{\mathbb{P}_{LoS}}(z) = \mathbb{P}\left[x_a \geq \frac{-2\ln z h_{max}(h_a - h_g)}{\lambda_0 (h_{max} - h_g)^2}\right] \tag{4.41}$$

Lets denote the right hand side fraction γ_2.

$$\gamma_2 = \frac{-2\ln z h_{max}(h_a - h_g)}{\lambda_0 (h_{max} - h_g)^2} \tag{4.42}$$

Once again we apply the Conditional Probability to the cdf in (4.39) and in respect to the transformation function that was found in(4.41)

$$F_{\mathbb{P}_{LoS}}(z) = \mathbb{P}\left[x_a \geq \gamma_1 \mid x_a \leq X\right]\mathbb{P}\left[x_a \leq X\right] + 1\mathbb{P}\left[x_a > X\right] \tag{4.43}$$

Similar steps as the previous case can be handled in this case. Finding the probability when $\mathbb{P}[x_a \leq X]$ which is the pdf of x_a and evaluating the integral from 0 to X.

$$\mathbb{P}[x_a \leq X] = \int_0^X \lambda_a e^{-\lambda_a y} dy = 1 - e^{-\lambda_a X} \tag{4.44}$$

Furthermore, we can also obtain the $\mathbb{P}[x_a > X]$ by plugging in (4.44)

$$\mathbb{P}[x_a > X] = 1 - \mathbb{P}[x_a \leq X] = e^{-\lambda_a X} \tag{4.45}$$

The Conditional Probability is calculated accordingly

$$\mathbb{P}\left[x_a \geq \gamma_1 \mid x_a \leq X\right] = \frac{\mathbb{P}\left[x_a > \gamma_1 \cap x_a \leq x\right]}{\mathbb{P}[x_a \leq X]} \tag{4.46}$$

Using similar methods as earlier from (4.32) to (4.35) we obtain the conditional probability

$$\mathbb{P}\left[x_a \geq \gamma_2 \mid x_a \leq X\right] = \frac{e^{-\lambda_a \gamma_2} - e^{-\lambda_a x}}{1 - e^{-\lambda_a X}} \tag{4.47}$$

Now we can have cdf of the LoS Probability of the first unblocked UAV as exponential random variable

$$F_{\mathbb{P}_{LoS}}(z) = \begin{cases} e^{-\lambda_a \gamma_2} & \text{for } z \geq e^{\frac{-\lambda_0 X (h_{max} - h_g)^2}{2h_{max}(h_a - h_g)}} \\ \\ e^{-\lambda_a X} & \text{for } z < e^{\frac{-\lambda_0 X (h_{max} - h_g)^2}{2h_{max}(h_a - h_g)}} \end{cases} \tag{4.48}$$

4.3.2 Simulation and Analysis Validation

To validate the numerical results without loss of generality we assumed the user have no significant height $h_g = 0$. During each trial, the UAV will have a new random location each time. Given that random location of the UAV, we compute the Los probability using our analysis found in (4.10) and store it in a vector. Where the vector will contain a set of randomly generated LoS probability that will help show the empirical cdf of the LoS Probability. That is because our LoS probability is now a function of random variable. This process was repeated for 15 thousand trials for each data point reported.

Figure 4.4 shows obtaining the LoS probability against the empirical cdf of LoS probability as a function of random variable depends on the distance X. The density of the blockages is set to value $\lambda_0 = 1/100$. Where the mean of the uav is $\lambda_a = 1/100$. The blockages have a maximum height of $h_{max} = 20$ (m) with LoS. The UAV is deployed randomly over the random distance of $X = 100$ (m) with a fixed altitude of $h_a = 80$ (m). As shown in figure 4.4 the user may connect to the UAV if $\mathbb{P}_{loS} > 0.8$. Also, there are two curves plotted, the

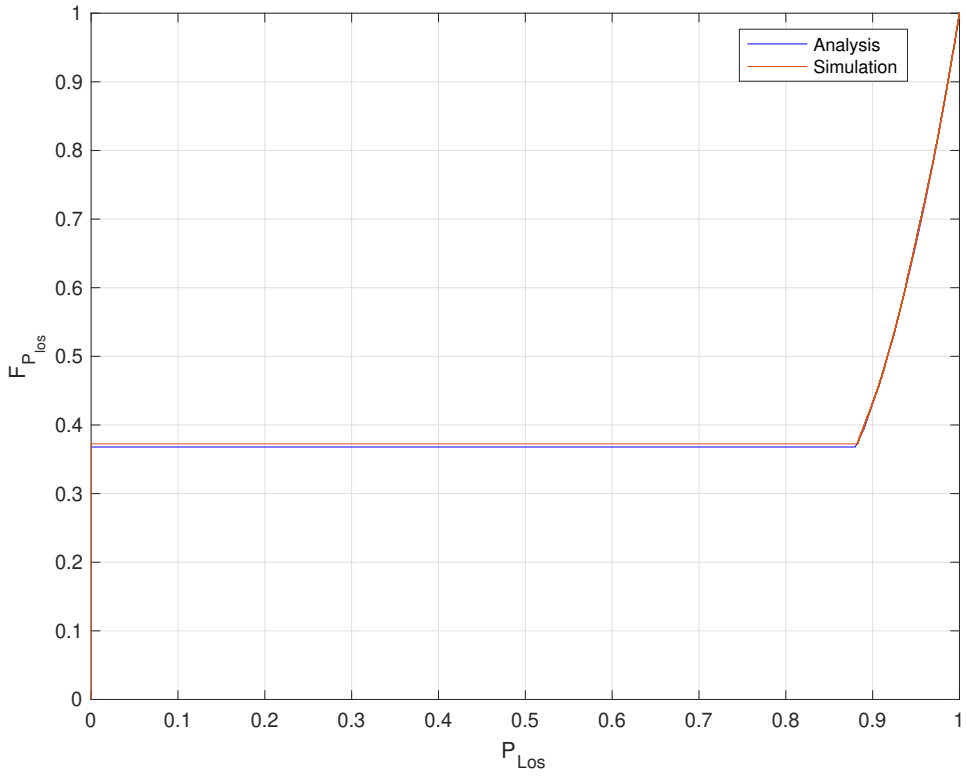

Figure 4.4: The empirical cumulative distribution function (CDF) of $\mathbb{P}_{LoS}$ over 15000 trial network realization

blue curve represents our analysis and the red curve represents our simulation. As shown in 4.4 we were able to successfully validate our analysis with simulation.

Figure 4.5 shows obtaining the LoS probability against the empirical cdf of LoS probability as a function of random variable depends on the distance x. The density of the blockages is $\lambda_0 = 1/60$. The mean of the UAV is $\lambda_a = 1/110$. The UAV is deployed randomly over the random distance of $x = 200$ (m) with a fixed altitude of $h_a = 80$ (m). In this figure, we parameterize over different height of the blockages with LoS $h_{max} = [20, 50, 100]$. As shown in figure 4.5 when h_{max} decreases the $\mathbb{P}_{LoS}$ increases. The reason is that potentially the height of the blockages is not obstructing the height of the UAV h_a. We can see the yellow curves shows the case where the is no LoS between the ground user to the UAV. The reason is that the h_{max} is now exceeding the height of the UAV.

Figure 4.6 shows obtaining the LoS probability against the empirical cdf of LoS probabil-

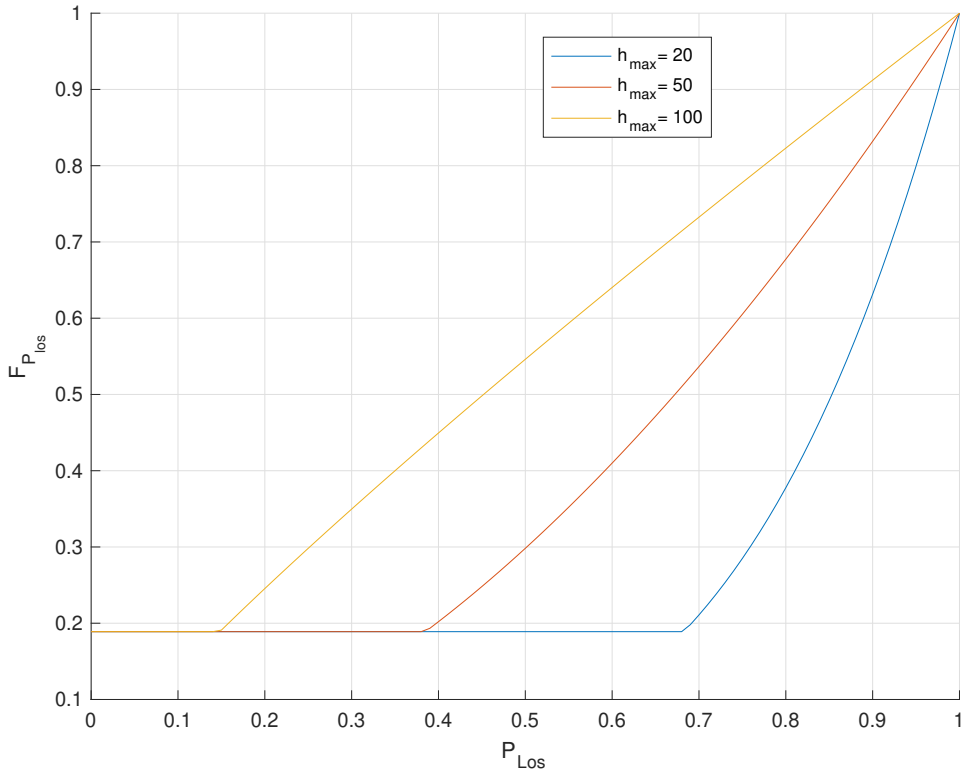

Figure 4.5: The empirical cumulative distribution function (CDF) of $\mathbb{P}_{LoS}$ over 15000 trial network realization.We parameterized over different maximum height of the blockages within LoS h_{max}

ity as a function of random variable depends on the distance x. The density of the blockages is $\lambda_0 = 1/60$. The mean of the UAV is $\lambda_a = 1/110$. The UAV is deployed randomly along the horizontal coordinate of $x = 200$ (m) with a fixed altitude of $h_a = 80$ (m). In this figure, we parameterize over different density of the blockages $\lambda_0 = [1/20, 1/50, 1/100]$. As shown in figure 4.6 when λ_0 increases the $\mathbb{P}_{LoS}$ decreases. The reason is that potentially there are more blockages that obstruct the connection between the ground user to the UAV.

Figure 4.7 shows obtaining the LoS probability against the empirical cdf of LoS probability as a function of random variable depends on the distance X. The density of the blockages is set to value $\lambda_0 = 1/100$. Where the mean of the UAV is $\lambda_a = 1/100$. The blockages have a maximum height of $h_{max} = 20$ (m) with LoS. The UAV is deployed randomly over the random distance of $x = 100$ (m). This is a cdf plot of LoS Probability parameterized over different heights of the UAV h_a. As shown in figure 4.7 the yellow curve indicates that the

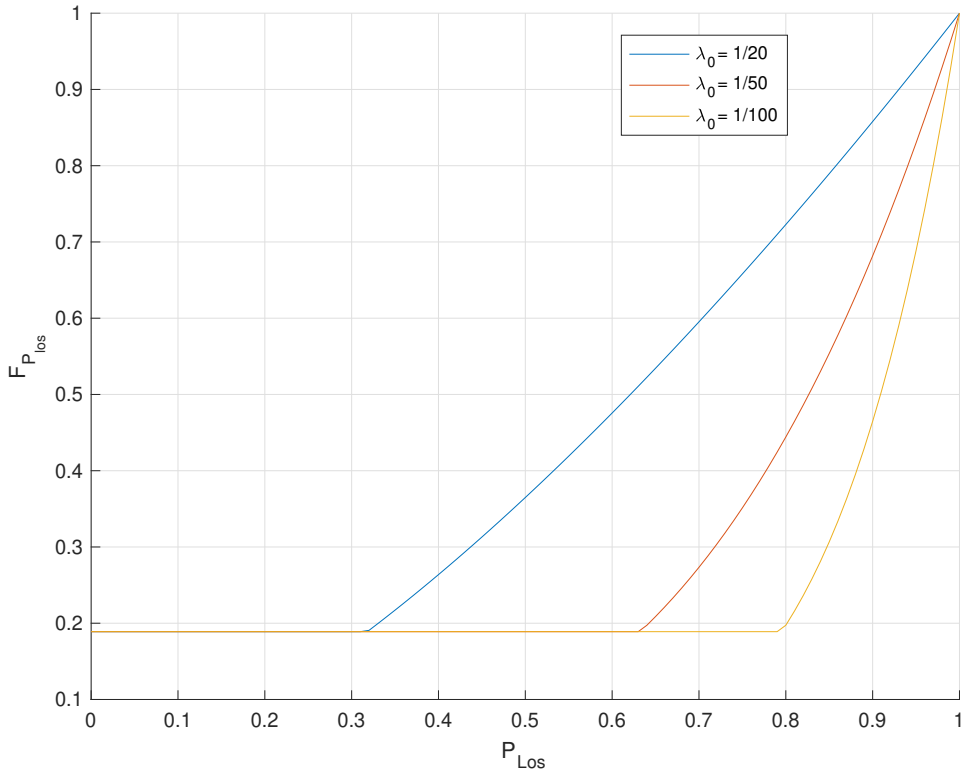

Figure 4.6: The empirical cumulative distribution function (CDF) of $\mathbb{P}_{LoS}$ over 15000 trial network realization. We have parameterized over different densities of the blockages λ_0

highest LoS probability that a UAV could have.

In order to find the optimal altitude the UAV could obtain the LoS we need find the optimal value of line of sight where the UAV could have direct LoS link with the user located at the ground. In figure 4.7 we have found that around the LoS probability of 0.8 the UAV have the best link with the user by simulation .Therefore in this figure 4.8 we have parameterized the altitude of the UAV $h_a = [10 : 5 : 180]$. The blockage density $\lambda_0 = 1/100$, and the UAV has a mean of $\lambda_a = 1/100$ as well. The blockages have a maximum height of $h_{max} = 20$ (m) with LoS. Since this was found through simulation it is important to note that the horizontal distance is now denoted by $R = 200(m)$. In addition,the transmission distance from the user located at the ground to the height of the UAV is denoted by $D = \sqrt{R^2 - h_a^2}$ that was computed in simulation.

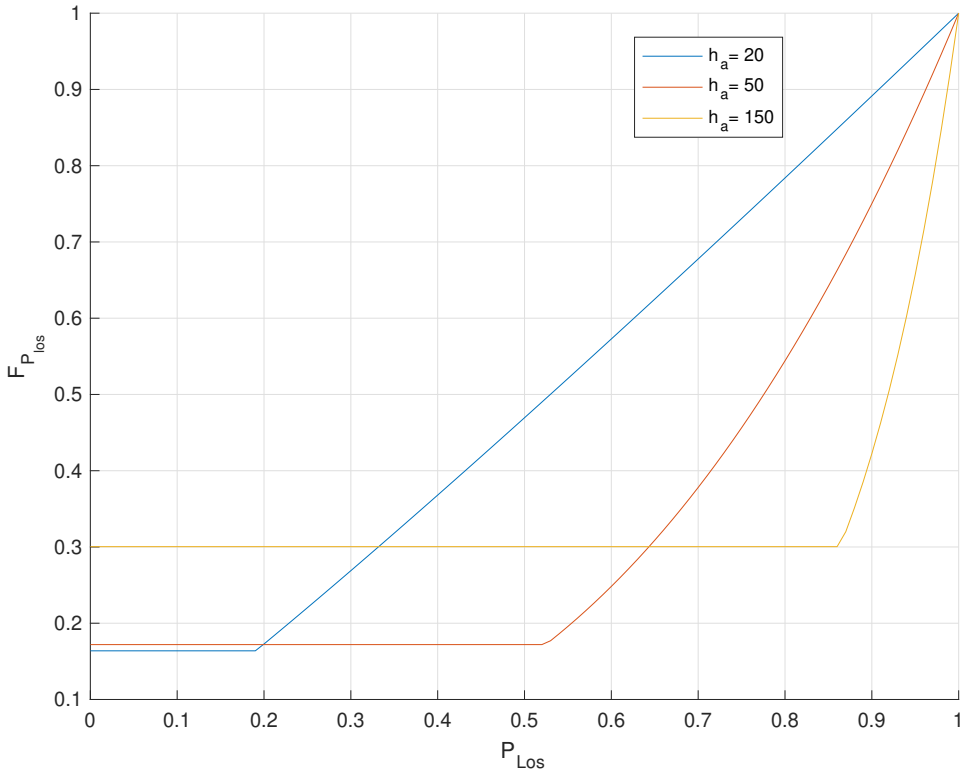

Figure 4.7: The empirical cumulative distribution function (CDF) of $\mathbb{P}_{LoS}$ parameterized over different UAV heights

4.4 Summary

To summarize, we looked at various scenarios of randomly deploying a single UAV over a one-dimensional network in this chapter. In terms of random UAV deployment, two instances were taken into consideration. The first instance of Uniform distribution. The exponential distribution was the second scenario. Additionally, we were able to understand that the LoS probability is a function of a random variable that depends on the UAV distance. Although the dependence of LoS probability was discussed in chapter 2, we were able to further explain how the position of the UAV will affect the LoS probability in this chapter. Additionally, we were able to use our simulation to verify the analysis. Finally, we were able to determine the UAV's optimal height at a high LoS probability value. While the deployment of one random UAV was the main emphasis of this chapter. Since we assumed that the first unblocked UAV is exponential, our work might be expanded to include multiple random UAVs.

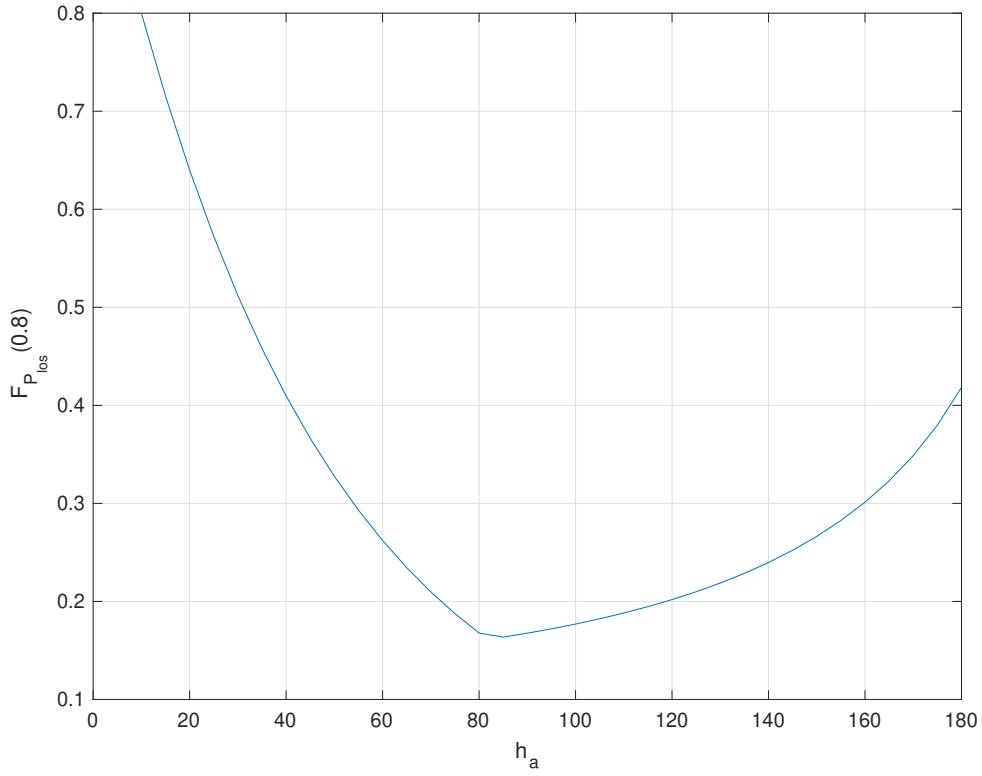

Figure 4.8: Optimal empirical cumulative distribution function (CDF) of $\mathbb{P}_{LoS}$ at 0.8. Where the distance to the first unblocked UAV is exponential x_a

.

Chapter 5

Conclusion

5.1 Summary and Future Work

In chapter (2), we found a closed-form analytical expression of the LoS probability in a wireless network when the blockages are drawn from a one-dimensional PPP. The number of blockages are Poisson random variable and their locations are independently distributed uniformly. However the blockages height varied in distributions. In addition, We can compute the LoS probability in respect to random blockages height in Uniform and Truncated Gaussian distribution. Some of the limitations that could be considered for the future work is to extend the work in finding the optimal height of the fixed UAV.

In chapter (3), we have extended our work found in (2) and considered a method to compute the LoS probability when the air asset is available to aid in the communication of between two ground assets in a Poisson forest environment with trees as random blockages distributed uniformly. In addition, to characterize the quality of the existing LoS links between assets we have calculated the throughput. The focus on this chapter was relaying the UAV communication between the two ground assets. By the proposed methodology found, we can extend the work with flexibility of the UAV. The mobility of the UAV along the horizontal distance or vertical distance which is basically the altitude of the UAV, when recognizing a potential obstruction to the signal.

Finally in chapter (4), we have extended our analysis found in chapters (2) and (3) to consider a new assumption of deploying a random UAV in a wireless network. The

deployment of the UAV were under two cases, the first case is considering one UAV uniformly distributed in a network and the second case is based on our observation of the uniform distribution case into accommodating our analysis to the possibility of multiple UAVs and the first UAV with LoS with ground user is exponential. Although, in the second case we have explored the case of multiple UAVs some of the limitations we found is that the multiple UAVs all share the same height. Therefore, for the future work we can see that with multiple UAVs we can extend the work found to two-dimensional network. In addition, the UAVs can be characterized by height distributions. Where the UAV could be randomly deployed but also the heights could be random.

References

[1] Y. Zeng, R. Zhang, and T. J. Lim, "Wireless communications with unmanned aerial vehicles: Opportunities and challenges," *IEEE Communications magazine*, vol. 54, no. 5, pp. 36–42, 2016.

[2] L. Liu, S. Zhang, and R. Zhang, "Comp in the sky: Uav placement and movement optimization for multi-user communications," *IEEE Transactions on Communications*, vol. 67, no. 8, pp. 5645–5658, 2019.

[3] M. Mozaffari, W. Saad, M. Bennis, and M. Debbah, "Unmanned aerial vehicle with underlaid device-to-device communications: Performance and tradeoffs," *IEEE Transactions on Wireless Communications*, vol. 15, no. 6, pp. 3949–3963, 2016.

[4] A. A. Deshpande, C. J. Vaca-Rubio, S. Mohebi, D. Salami, E. de Carvalho, P. Popovski, S. Sigg, M. Zorzi, and A. Zanella, "Energy-efficient design for ris-assisted uav communications in beyond-5g networks," in *2022 20th Mediterranean Communication and Computer Networking Conference (MedComNet)*. IEEE, 2022, pp. 158–165.

[5] W. Khawaja, I. Guvenc, D. W. Matolak, U.-C. Fiebig, and N. Schneckenburger, "A survey of air-to-ground propagation channel modeling for unmanned aerial vehicles," *IEEE Communications Surveys & Tutorials*, vol. 21, no. 3, pp. 2361–2391, 2019.

[6] A. Fotouhi, H. Qiang, M. Ding, M. Hassan, L. G. Giordano, A. Garcia-Rodriguez, and J. Yuan, "Survey on uav cellular communications: Practical aspects, standardization advancements, regulation, and security challenges," *IEEE Communications Surveys & Tutorials*, vol. 21, no. 4, pp. 3417–3442, 2019.

[7] M. Mozaffari, W. Saad, M. Bennis, Y.-H. Nam, and M. Debbah, "A tutorial on uavs for wireless networks: Applications, challenges, and open problems," *IEEE communications surveys & tutorials*, vol. 21, no. 3, pp. 2334–2360, 2019.

[8] Q. Wu, Y. Zeng, and R. Zhang, "Joint trajectory and communication design for multi-uav enabled wireless networks," *IEEE Transactions on Wireless Communications*, vol. 17, no. 3, pp. 2109–2121, 2018.

[9] E. Hriba, M. C. Valenti, and R. W. Heath, "Optimization of a millimeter-wave uav-to-ground network in urban deployments," in *MILCOM 2021-2021 IEEE Military Communications Conference (MILCOM)*. IEEE, 2021, pp. 861–867.

[10] H. R. Hussen, S.-C. Choi, J.-H. Park, and I.-Y. Ahn, "Efficient multi-uav relay nodes placement scheme in wireless networks," in *2021 International Conference on Information and Communication Technology Convergence (ICTC)*. IEEE, 2021, pp. 893–898.

[11] T. S. Rappaport, S. Sun, R. Mayzus, H. Zhao, Y. Azar, K. Wang, G. N. Wong, J. K. Schulz, M. Samimi, and F. Gutierrez, "Millimeter wave mobile communications for 5g cellular: It will work!" *IEEE access*, vol. 1, pp. 335–349, 2013.

[12] P. Wang, M. Ozger, C. Cavdar, and M. Petrova, "Beyond visual line of sight piloting of uavs using millimeter-wave cellular networks," in *2019 IEEE 30th Annual International Symposium on Personal, Indoor and Mobile Radio Communications (PIMRC)*. IEEE, 2019, pp. 1–7.

[13] J. G. Andrews, T. Bai, M. N. Kulkarni, A. Alkhateeb, A. K. Gupta, and R. W. Heath, "Modeling and analyzing millimeter wave cellular systems," *IEEE Transactions on Communications*, vol. 65, no. 1, pp. 403–430, 2016.

[14] I. Mohammed, I. B. Collings, and S. V. Hanly, "Line of sight probability prediction for uav communication," in *2021 IEEE International Conference on Communications Workshops (ICC Workshops)*. IEEE, 2021, pp. 1–6.

[15] E. Hriba, "Analysis of millimeter-wave networks: Blockage, antenna directivity, macrodiversity, and interference," Ph.D. dissertation, West Virginia University, 2021.

[16] M. Di Renzo, "Stochastic geometry modeling and analysis of multi-tier millimeter wave cellular networks," *IEEE Transactions on Wireless Communications*, vol. 14, no. 9, pp. 5038–5057, 2015.

[17] T. Bai, R. Vaze, and R. W. Heath, "Analysis of blockage effects on urban cellular networks," *IEEE Transactions on Wireless Communications*, vol. 13, no. 9, pp. 5070–5083, 2014.

[18] M. A. Ouamri, "Stochastic geometry modeling and analysis of downlink coverage and rate in small cell network," *Telecommunication Systems*, vol. 77, no. 4, pp. 767–779, 2021.

[19] T. Bai and R. W. Heath, "Coverage and rate analysis for millimeter-wave cellular networks," *IEEE Transactions on Wireless Communications*, vol. 14, no. 2, pp. 1100–1114, 2014.

[20] K. Venugopal, M. C. Valenti, and R. W. Heath, "Device-to-device millimeter wave communications: Interference, coverage, rate, and finite topologies," *IEEE Transactions on Wireless Communications*, vol. 15, no. 9, pp. 6175–6188, 2016.

[21] J. Zhang and J. G. Andrews, "Distributed antenna systems with randomness," *IEEE Transactions on Wireless Communications*, vol. 7, no. 9, pp. 3636–3646, 2008.

[22] M. Haenggi, *Stochastic Geometry for Wireless Networks*. Cambridge University Press, 2012.

[23] M. C. Valenti, D. Torrieri, and S. Talarico, "A direct approach to computing spatially averaged outage probability," *IEEE Commun. Letters*, vol. 18, no. 7, pp. 1103–1106, July 2014.

[24] A. Leon-Garcia, *Probability, Statistics, and Random Processes for Electrical Engineering, 3rd ed.* Upper Saddle River: Pearson, 2008.

[25] I. S. Gradshteyn and I. M. Ryzhik, *Table of Integrals, Series, and Products.* Academic press, 2014.

[26] T. S. Rappaport, S. Sun, R. Mayzus, H. Zhao, Y. Azar, K. Wang, G. N. Wong, J. K. Schulz, M. Samimi, and F. Gutierrez, "Millimeter wave mobile communications for 5g cellular: It will work!" *IEEE Access*, vol. 1, pp. 335–349, 2013.

[27] Y. Rahayu and M. I. Hidayat, "Design of 28/38 GHz dual-band triangular-shaped slot microstrip antenna array for 5G applications," in *International Conference on Telematics and Future Generation Networks (TAFGEN)*, 2018, pp. 93–97.